

A Review of Bayesian Uncertainty Quantification in Deep Probabilistic Image Segmentation

Amaan Valiuddin

Ruud van Sloun

Christiaan Viviers

Peter de With

Fons van der Sommen

Department of Electrical Engineering

Eindhoven University of Technology

m.m.a.valiuddin@tue.nl

r.g.j.sloun@tue.nl

c.g.a.viviers@tue.nl

p.h.n.de.with@tue.nl

fvdsmomen@tue.nl

Abstract

Advances in architectural design, data availability, and compute have driven remarkable progress in semantic segmentation. Yet, these models often rely on relaxed Bayesian assumptions, omitting critical uncertainty information needed for robust decision-making. The resulting reliance on point estimates has fueled interest in probabilistic segmentation, but the literature remains fragmented. In response, this review consolidates and contextualizes foundational concepts in uncertainty modeling, including the non-trivial task of distinguishing between epistemic and aleatoric uncertainty and examining their roles across four key downstream segmentation tasks, highlighting Active Learning as particularly promising. By unifying theory, terminology, and applications, we provide a coherent foundation for researchers and identify critical challenges, such as strong assumptions in spatial aggregation, lack of standardized benchmarks, and pitfalls in current uncertainty quantification methods. We identify trends such as the adoption of contemporary generative models, driven by advances in the broader field of generative modeling, with segmentation-specific innovation primarily in the conditioning mechanisms. Moreover, we observe growing interest in distribution- and sampling-free approaches to uncertainty estimation. We further propose directions for advancing uncertainty-aware segmentation in deep learning, including pragmatic strategies for disentangling different sources of uncertainty, novel uncertainty modeling approaches and improved Transformer-based backbones. In this way, we aim to support the development of more reliable, efficient, and interpretable segmentation models that effectively incorporate uncertainty into real-world applications.

1 Introduction

Image segmentation entails pixel-wise classification of data, effectively delineating objects and regions of interest (Szeliski, 2010). The advent of convolutional neural networks (CNNs) has led to major breakthroughs in this domain, with deep learning-based methods achieving state-of-the-art performance on large-scale datasets (Ronneberger et al., 2015; Shelhamer et al., 2014; Badrinarayanan et al., 2015), obtaining impressive scores with large-scale segmentation datasets (Lin et al., 2014; Cordts et al., 2016b; Richter et al., 2016). However, these models typically rely on strong assumptions and significant relaxations of the Bayesian learning paradigm, neglecting the uncertainty associated with their predictions. This lack of uncertainty modeling reduces both the reliability and interpretability of the predictions. In high-stakes applications, such as autonomous driving or medical diagnosis, this can have severe consequences. For instance, misclassifying adjacent objects in autonomous driving or overlooking uncertainty in lesion classification can both lead to critical decision-making errors.

Fortunately, the merits of uncertainty quantification have been well-recognized in the field of CNN-based segmentation, especially as interpretability and reliability have become central in data-driven applications.

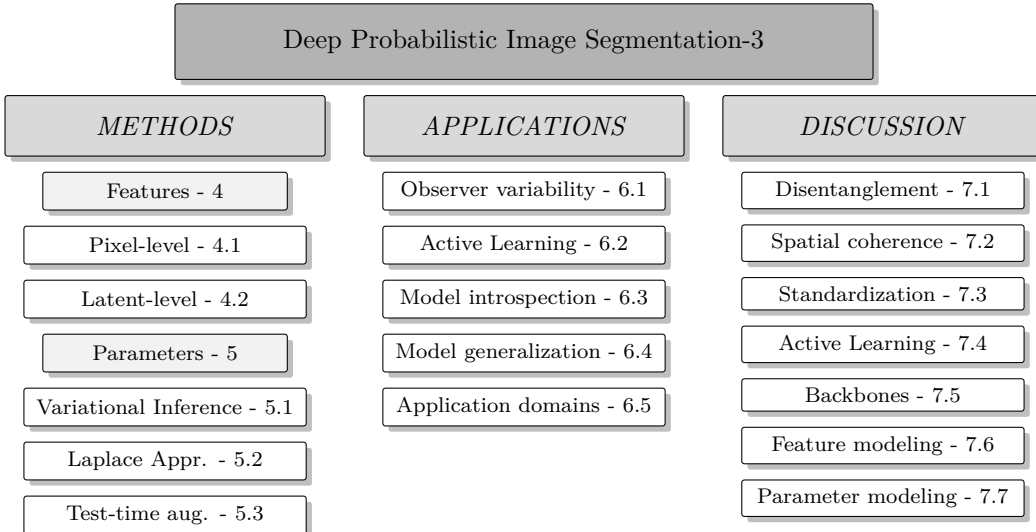


Figure 1: Overview of the sections. The leafs of the presented hierarchical tree are related to subsections of the article.

Extensive efforts have been made to align neural network optimization with Bayesian machine learning (Blundell et al., 2015; Guo et al., 2017; Kingma & Welling, 2013; Kendall & Gal, 2017), such as learning parameter distributions rather than point estimates to capture *epistemic* uncertainty. Additionally, explicitly modeling the likelihood of outputs enables estimation of *aleatoric* uncertainty. However, in practice, these two forms of uncertainty are often entangled or even conflicting (Mucsányi et al., 2024; de Jong et al., 2024; Valdenegro-Toro & Mori, 2022; Hüllermeier & Waegeman, 2021), making the distinction difficult to define and apply. This conceptual ambiguity presents significant barriers to understanding and implementation (Kahl et al., 2024; Der Kiureghian & Ditlevsen, 2009; Kirchhof et al., 2025). At the same time, uncertainty is often treated as an auxiliary tool to enhance downstream performance, rather than as a primary modeling objective. As a result, many works lack rigorous theoretical grounding, focusing instead on empirical gains without clear definitions or principled formulations of uncertainty. Furthermore, many approaches are tailored to specific datasets or modalities, limiting generalizability. Moreover, theoretical contributions often originate from adjacent fields like Bayesian deep learning or information theory, and can be insufficiently contextualized within the domain of segmentation. This disconnect has resulted in a fragmented body of work, with inconsistent terminology, evaluation metrics, and assumptions. The resulting abundance of literature can be overwhelming, even for experienced researchers.

This paper aims to explore and clarify these concepts in the context of segmentation architectures and their impact on downstream tasks. Given these challenges and the renewed interest in uncertainty (Papamarkou et al., 2024; Kirchhof et al., 2025), we note that a comprehensive overview in the field remains limited. Due to its application-driven nature, most existing surveys adopt a medical perspective (Jungo & Reyes, 2019; Kwon et al., 2020), often focused on specific modalities (McCrindle et al., 2021; Jungo et al., 2020; Ng et al., 2022; Roshanzamir et al., 2023). However, the connection between theoretical foundations and their diverse applications remains underexplored. Additionally, the study by Kahl et al. (2024) introduces a valuable framework for benchmarking uncertainty disentanglement in semantic segmentation, but focuses primarily on empirical evaluation within specific tasks. In contrast, our work provides a comprehensive overview that spans the full range of established uncertainty quantification methods, unifies and contextualizes the underlying theory, and standardizes terminology and notation. This broader perspective helps clarify conceptual foundations and highlights cross-cutting insights across segmentation architectures and application domains. By the end of this paper, readers will have a clear understanding of the various forms of uncertainty, their relevance to segmentation tasks, and a comprehensive grasp of the key challenges and open research directions in the field.

This review paper is structured as follows. Past work with significant impact in general image segmentation is presented in Section 2. Then, the theoretical framework and notation that govern the remainder of the paper are introduced in Section 3. The theory enables us to classify the approaches into two distinct but often related methods. That is, methods targeting either aleatoric or epistemic uncertainty, which can be distinguished by either modeling the feature or parameter distribution(s). The role of these concepts in image segmentation are treated in Sections 4 and 5, respectively, which include all architectures and approaches with significant impact on the field. We then correlate these modeling methods to specific applications in Section 6. Here, we also observe for which domains uncertainty quantification has been exploited. Then, this overview is discussed further in Section 7. This section is particularly valuable for researchers seeking to identify the most suitable model for their specific segmentation task. To encourage further research in this field, we provide future recommendations by highlighting key challenges, gaps and pitfalls in literature, concluding our review in Section 8. Figure 1 illustrates a brief overview of the sections.

2 Background

A common approach in image understanding involves labeling pixels according to semantic categories, which is the core of *semantic segmentation*. This technique is particularly well-suited for amorphous or uncountable subjects. In contrast, *instance segmentation* not only assigns class labels, but also distinguishes and delineates individual object occurrences. This makes it more appropriate for scenarios involving countable entities. A third variant, *panoptic segmentation*, unifies both semantic and instance-level labeling, offering a comprehensive view of scene composition. As summarized by Minaee et al. (2020), semantic segmentation has been performed using methods such as thresholding (Otsu, 1979), histogram-based bundling, region-growing (Dhanachandra et al., 2015), k-means clustering (Nock & Nielsen, 2004), watershedding (Najman & Schmitt, 1994), to more advanced algorithms such as active contours (Kass et al., 2004), graph cuts (Boykov et al., 2001), conditional and Markov random fields (Plath et al., 2009), and sparsity-based methods (Starck et al., 2005; Minaee & Wang, 2017). While the literature on segmentation is vast and rapidly evolving, a selection of backbone architectures has been particularly influential in shaping current probabilistic segmentation models. The focus here is not on exhaustiveness, but on those models most relevant to the development of uncertainty-aware approaches.

In particular, following the successful application of CNNs (LeCun et al., 1998), image segmentation experienced rapid progress driven by increasingly powerful and specialized deep architectures. Notably, the Fully Convolutional Network (FCN) (Shelhamer et al., 2014) adapted the AlexNet (Krizhevsky et al., 2012), VGG16 (Simonyan & Zisserman, 2014) and GoogLeNet (Szegedy et al., 2014) architectures to enable end-to-end semantic segmentation. Furthermore, other CNN architectures such as DeepLabv3 (Chen et al., 2017), and the MobileNetv3 (Howard et al., 2019) have also been commonly used. As the research progressed, increasing success has been observed with encoder-decoder models (Noh et al., 2015; Badrinarayanan et al., 2015; Yuan et al., 2019; Ronneberger et al., 2015). Initially developed for the medical applications, Ronneberger Ronneberger et al. (2015) introduced the U-Net, which successfully relies on residual connections between the encoding-decoding path, to preserve high-frequency details in the encoded feature maps. To this day, the U-Net is still often utilized as the default backbone model for many semantic segmentation and even general image generation architectures (Ho et al., 2020; Song et al., 2020), particularly in the medical domain. In fact, reports of recent research indicate that the relatively simple U-Net (Isensee et al., 2020) still outperform more contemporary and complex models (Eisenmann et al., 2023; Isensee et al., 2024).

3 Probabilistic Image Segmentation

Assuming random-variable pairs $(\mathbf{Y}, \mathbf{X}) \sim P_{Y,X}$ that take values in $\mathcal{Y} \in \mathbb{Z}^{K \times H \times W}$ and $\mathcal{X} \in \mathbb{R}^{C \times H \times W}$, respectively, then instance \mathbf{y} can be considered as the ground-truth of a K -class segmentation task and instance \mathbf{x} as the query image. The variables H , W and C correspond to the image height, width and channel depth, respectively. Conforming to the principle of maximum entropy, the optimal parameters given the data (i.e. posterior) subject to the chosen intermediate distributions can be inferred through Bayes

Theorem as

$$p(\boldsymbol{\theta}|\mathbf{y}, \mathbf{x}) = \frac{p(\mathbf{y}|\mathbf{x}, \boldsymbol{\theta})p(\boldsymbol{\theta})}{p(\mathbf{y}|\mathbf{x})}, \quad (1)$$

assuming independence of \mathbf{x} from $\boldsymbol{\theta}$, and where $p(\boldsymbol{\theta})$ represents the prior belief on the parameter distribution and $p(\mathbf{y}|\mathbf{x})$ the conditional data likelihood (also commonly referred to as the *evidence*). After obtaining a posterior with dataset $\mathcal{D} = \{\mathbf{x}_i, \mathbf{y}_i\}_{i=1}^N$ containing N images, the predictive distribution from a new datapoint \mathbf{x}^* can be denoted as

$$p(\mathbf{Y}|\mathbf{x}^*, \mathcal{D}) = \underbrace{\int}_{\text{Data}} \underbrace{p(\mathbf{Y}|\mathbf{x}^*, \boldsymbol{\theta})}_{\text{Model}} \underbrace{p(\boldsymbol{\theta}|\mathcal{D})}_{\text{Posterior}} d\boldsymbol{\theta}. \quad (2)$$

As evident, both the variability in the empirical data and the inferred parameters of the model influence the predictive distribution. Hence, uncertainties stemming from the conditional likelihood distribution are classified as either *aleatoric*, implying from the statistical diversity in the data, or *epistemic*, which stems from the posterior, i.e. the variance of the model parameters. Encapsulating a particular uncertainty can therefore be achieved by incorporating parametrized stochasticity at either feature- or parameter-level. A straightforward approach to quantify any of these uncertainties is achieved by obtaining the predictive entropy, $H[\mathbf{Y}|\mathbf{x}^*, \mathcal{D}]$, i.e. the entropy of the predictive distribution $p(\mathbf{Y}|\mathbf{x}^*, \mathcal{D})$. Furthermore, disentangling these uncertainties can be achieved through its decomposition

$$H[\mathbf{Y}|\mathbf{x}^*, \mathcal{D}] = \underbrace{I[\mathbf{y}, \boldsymbol{\theta}|\mathbf{x}^*, \mathcal{D}]}_{\text{epistemic}} + \underbrace{\mathbb{E}_{q(\boldsymbol{\theta}|\mathcal{D})}[H[\mathbf{y}|\mathbf{x}^*, \boldsymbol{\theta}]]}_{\text{aleatoric}}, \quad (3)$$

where I represents the mutual information. In this way, it is theoretically possible to identify whether high-entropy predictions are due to model ignorance or statistical ambiguity inherent in the data generating process. Nonetheless, determining the nature of uncertainty is not often straightforward. For example, Hüllermeier & Waegeman (2021) stated that “*by allowing the learner to change the setting, the distinction between these two types of uncertainty will be somewhat blurred*”. This sentiment is also shared by Der Kiureghian & Ditlevsen (2009), noting that “*in one model an addressed uncertainty may be aleatory, in another model it may be epistemic*”. Sharing similar views, we highlight the necessity of careful analyses and possible subjective interpretation regarding the topic as we treat the realm of quantifying spatially correlated uncertainty. Especially with increasingly complex methodologies, treating the uncertainties as separate concepts is mostly theoretical (often even more philosophical) and highly non-trivial in practice.

3.1 Conventional segmentation

Regardless of the elegantly formulated Bayesian posterior, most practical approaches make use of so-called “deterministic” segmentation networks, which are trained by Maximum Likelihood Estimation (MLE) and is specified as

$$\boldsymbol{\theta}_{\text{MLE}} = \arg \max_{\boldsymbol{\theta}} \log p(\mathbf{y}|\mathbf{x}, \boldsymbol{\theta}), \quad (4)$$

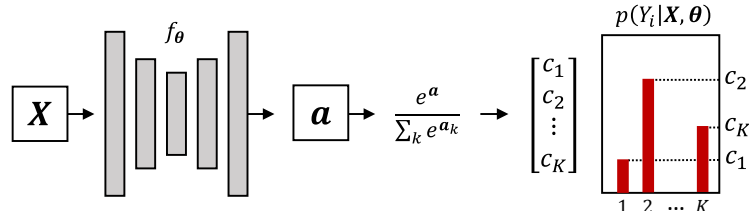


Figure 2: Aleatoric uncertainty quantification by modeling pixel-level outputs as parameters of a Probability Mass Function.

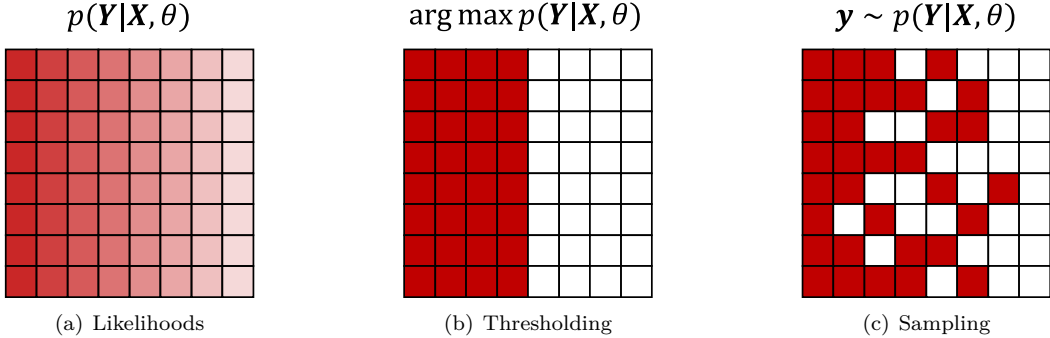


Figure 3: Illustration of the likelihood function in segmentation models. Color intensities reflect the normalized confidence values that can be interpreted as probabilities. (a) The continuous output results in a horizontal gradient. (b) Maximum likelihood thresholding can be applied. (c) However, the coherence of the segmentation suffers when sampling.

which simplifies the training procedure by taking a point estimate of the posterior. This approximation improves as the training data increases and the model parameter variances approach zero. As such, MLE does not include any prior knowledge on the structure of the parameter distribution but can be achieved through Maximum A Posteriori (MAP) estimation with

$$\boldsymbol{\theta}_{\text{MAP}} = \arg \max_{\boldsymbol{\theta}} \log p(\mathbf{y}|\mathbf{x}, \boldsymbol{\theta}) + \log p(\boldsymbol{\theta}). \quad (5)$$

For example, assuming Gaussian or Laplacian priors leads to regularizing the L_2 norm (also known as *ridge regression* or *weight decay*) or L_1 norm of $\boldsymbol{\theta}$, respectively (Figueiredo, 2001; Kaban, 2007). To model $p(\mathbf{y}|\mathbf{x}, \boldsymbol{\theta})$, we make use of function $f_{\boldsymbol{\theta}} : \mathbb{R}^{C \times D} \rightarrow \mathbb{R}^{K \times D}$ that infers the parameters of a Probability Mass Function (PMF). For instance, consider spatial image dimensions D and a CNN with $\mathbf{a} = f_{\boldsymbol{\theta}}(\mathbf{x})$. Then, we can write

$$p(\mathbf{Y} = k \mid \mathbf{x}^*, \boldsymbol{\theta}) = \frac{e^{\mathbf{a}_k}}{\sum_k e^{\mathbf{a}_k}}, \quad (6)$$

with channel-wise indexing over the denominator, which is commonly known as the SoftMax activation (Figure 2). This approach is probabilistic modeling in the technical sense, although it is not referred to as such in common nomenclature. In fact, the approximated distribution can represent and localize uncertain regions. However, the implicit pixel-independence assumption

$$p(\mathbf{Y}|\mathbf{X}) = \prod_i^{K \times D} p(Y_i|\mathbf{X}), \quad (7)$$

omits information on structural variation in the segmentation masks. In conventional classification, factorizing the categorical distribution is typically regarded as a logical simplification. In probabilistic segmentation however, this assumption has caused the emergence of a distinct research direction (See Figure 3). The challenge of sampling of spatially coherent segmentation masks can be addressed either from the aleatoric or epistemic perspective, usually indicating reducibility of the assumed uncertainty source. Both approaches have specific use cases, and each modeling choice comes with distinct advantages and limitations, which will be discussed in the following sections.

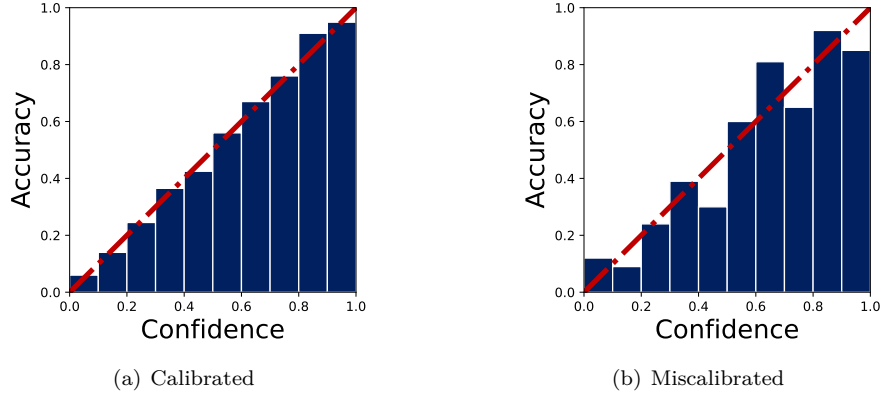


Figure 4: Visualization of a reliability diagram, which illustrates whether the model’s predicted confidences align with the observed empirical accuracies.

4 Feature modeling

Aleatoric uncertainty modeling reconsiders the non-deterministic relationship between $x \in \mathcal{X}$ and $y \in \mathcal{Y}$, which implies that

$$p(\mathbf{Y}|\mathbf{X}) = \frac{p(\mathbf{Y}, \mathbf{X})}{p(\mathbf{X})} \neq \delta(\mathbf{Y} - F(\mathbf{X})), \quad (8)$$

with Dirac-delta function δ , and mapping $F : \mathcal{X} \rightarrow \mathcal{Y}$. This relationship is characterized by the ambiguity in \mathbf{X} and is inherently probabilistic, due to various reasons such as noise in the data (occlusions, sensor noise, insufficient resolution, etc.) or variability within a class (e.g. not all cats have tails). Hence, the observance of substantial aleatoric uncertainty can in some cases be inevitable, but may also signal the need for higher-quality data acquisition or shifting to another modality. The possible input dependency of the uncertainty develops into further categorization of either *heteroscedastic* (dependent) or *homoscedastic* (independent) aleatoric uncertainty. In most practical scenarios, aleatoric uncertainty modeling methods encompass both types and assume a parameterized likelihood function $p(\mathbf{Y}|\mathbf{X}, \theta)$ as a direct reflection of $p(\mathbf{Y}|\mathbf{X})$. For example, it is possible to model a distribution parameterized by the output of a CNN. Also, conditional generative models are used to learn the data distribution through so-called “latent” (i.e. unobserved) variables. For the purpose of taxonomy, we categorize models based on the location of these latent variables: those introduced near the output are discussed in Section 4.1, while lower-dimensional latents embedded deeper within the architecture are covered in Section 4.2. While their theoretical formulations are largely similar, their practical implications can differ significantly.

4.1 Pixel-level sampling

Uncertainty in segmentation masks can be modeled directly at the pixel level. These approaches can be further categorized into those that assume independence between pixels (Section 4.1.1), and those that explicitly model spatial correlations (Section 4.1.2). In the former case, accurate uncertainty estimates rely on well-calibrated models, which is an assumption that often fails in practice without additional tuning on a separate calibration set. In the latter case, a stochastic variable is introduced to capture dependencies between neighboring pixels.

4.1.1 Independence

As discussed earlier, neural network predictions are often normalized with SoftMax activation in order to interpret the confidence values as parameters of a probability mass distribution, but rarely reflect the true probabilities in modern neural networks Guo et al. (2017). Thus, interpreting the confidences as true probabilities is often only justified after proper validation, which is referred to as *model calibration*. Here, it is measured whether the empirical accuracy of a model approximately equals the provided class confidence

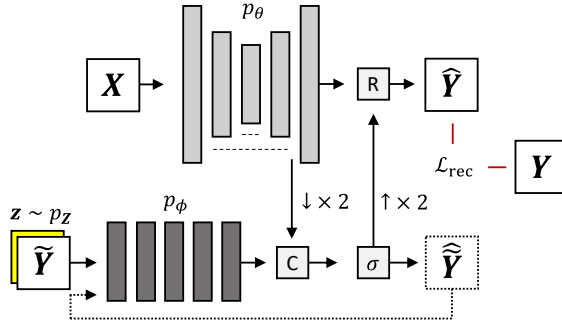


Figure 5: Illustration of the PixelCNN-based PixelSeg (Zhang et al., 2022c). Parameter ‘C’ indicates the concatenation module, ‘R’ the resampling module and σ the softmax activation. Dotted elements appear during test-time sampling.

c_k for class k , i.e. $P(Y = k | c_k) = c_k$. Calibration is typically visualized with a reliability diagram, where miscalibration and under-/over-confidence can be assessed by inspecting the deviation from the graph diagonal (Figure 4). Furthermore, different methods can be used to quantify calibration, although each may introduce its own biases. A fairly straightforward metric, the Expected Calibration Error (ECE), determines the normalized distance between accuracy (acc) and confidence (conf) bins as

$$E_{\text{ECE}} = \sum_{b=1}^B \frac{n_b}{N} |\text{acc}(b) - \text{conf}(b)|, \quad (9)$$

with n_b the number of samples in bin b and N being the total sample size across all bins. The ECE is prone to skew representations if some bins are significantly more populated with samples due to over-/under-confidence. Furthermore, the Maximum Calibration Error (MCE) is more appropriate for high-risk applications, where only the worst bin is considered. Additionally, when background pixels have a predominant influence, each bin can be weighted equally using the Average Calibration Error (ACE) to mitigate this imbalance Jungo et al. (2020); Neumann et al. (2018).

Nonetheless, contemporary neural networks often exhibit poorly calibrated uncertainty estimates. This misalignment is hypothesized due to the use of negative log-likelihood as the training objective, along with regularization techniques such as batch normalization, weight decay, and others (Guo et al., 2017). As a result, calibration methods are typically required to adjust the predicted confidences. Since most of these techniques are post-hoc, i.e. applied after training, they necessitate a separate validation set. For example, Temperature Scaling (Guo et al., 2017) has been applied in a pixel-wise manner for segmentation problems (Ding et al., 2021). Nonetheless, some methods, such as Label Smoothing (Silva & Oliveira, 2021; Liu et al., 2022a) or using the Focal Loss (Mukhoti et al., 2020) can be directly applied on the training data. Furthermore, over-fitting has often been considered to be the cause of over-confidence (Szegedy et al., 2016; Pereyra et al., 2017) and erroneous pixels can therefore be penalized through regularizing low-entropy outputs (Larrazabal et al., 2021a).

4.1.2 Spatial correlation

Assuming pixel independence inhibits spatial coherence in uncertainty quantification, which is a key factor for segmentation. Introducing spatial correlation can be achieved through an autoregressive approach. For instance, we can rephrase Equation (7) to

$$p(Y|X) = \prod_i^{K \times D} p(Y_i|Y_1, \dots, Y_{i-1}, X), \quad (10)$$

where pixel Y_i is predicted based on the preceding pixels. A popular implementation of this formulation is known as the PixelCNN (Van Den Oord et al., 2016). For dense predictions, Zhang et al. (2022c) propose

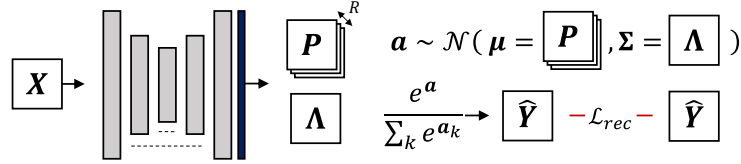


Figure 6: Depiction of Stochastic Segmentation Networks (Monteiro et al., 2020). Here, the covariance of the likelihood distribution is explicitly modeled through a low-rank approximation.

PixelSeg, which predicts a downsampled segmentation mask $\tilde{\mathbf{y}}$ with $p_\phi(\tilde{\mathbf{y}}|\mathbf{x})$, and fuse this with a conventional CNN to predict the full-resolution mask with $p_\theta(\mathbf{y}|\tilde{\mathbf{y}}, \mathbf{x})$. The two masks are fused through a resampling module, containing a series of specific transformations to improve quality and diversity of the samples. Figure 5 illustrates this concept. Notably, PixelCNNs employ a recursive sampling process, which also enables completion/inpainting of user-given inputs.

Monteiro et al. (2020) propose the Stochastic Segmentation Network (SSN), which models the output logits as a multivariate normal distribution, parameterized by the neural networks f_θ^μ and f_θ^Σ . Given the output features $f_\theta(\mathbf{x}) = \mathbf{a}$ of a deterministic model, we can denote the logits distribution as

$$p(\mathbf{a}|\mathbf{x}, \theta) = \mathcal{N}(\mathbf{a}; \mu = f_\theta^\mu(\mathbf{x}), \Sigma = f_\theta^\Sigma(\mathbf{x})), \quad (11)$$

where the covariance matrix has a low-rank structure $\Sigma = \mathbf{P}\mathbf{P}^T + \mathbf{\Lambda}$, with \mathbf{P} having dimensionality $((K \times D) \times R)$, with R being a hyperparameter that controls the parameterization rank and $\mathbf{\Lambda}$ representing a diagonal matrix. The low-rank assumption results in a more structured distribution, while retaining reasonable efficiency. Monte Carlo sampling is used to generate predictions, which are then mapped to categorical values using the SoftMax activation. SSNs can theoretically be augmented to any pretrained CNNs as an additional layer (see Figure 6).

4.2 Latent-level sampling

The limitation of modeling intricate, complex distributions directly at the output level can be mitigated by using generative models, which often rely on simpler, lower-dimensional latent variables $\mathbf{z} \sim p_\mathbf{z}$ with $\mathcal{Z} \in \mathbb{R}^d$, to instead learn the approximate through

$$p_{\theta, \psi}(\mathbf{Y}|\mathbf{X}) = \int p_\theta(\mathbf{Y}|\mathbf{z}, \mathbf{X}) p_\psi(\mathbf{z}|\mathbf{X}) d\mathbf{z}, \quad (12)$$

with parameters θ, ψ . As such, the spatial correlation is induced through mapping the latent variables to segmentation masks. Conditioning the latent density, i.e. $p_\psi(\mathbf{z}|\mathbf{X})$, on the input images is not a necessity, but usually preferred for smooth optimization trajectories Zheng et al. (2022). However, it is also possible to simply employ an unconditional prior $p(\mathbf{z})$. As argued by Kahl et al. (2024), their predictive uncertainty can be decomposed as

$$H[\mathbf{Y}|\mathbf{x}, \theta] = \underbrace{I[\mathbf{Y}, \mathbf{z}|\mathbf{x}, \theta]}_{\text{aleatoric}} + \overbrace{\mathbb{E}_{p(\mathbf{z})}[H[\mathbf{Y}|\mathbf{z}, \mathbf{x}, \theta]]}^{\text{epistemic}}. \quad (13)$$

In contrast to Equation (3), the mutual information term here encapsulates the aleatoric uncertainty, while the expected entropy reflects the epistemic uncertainty. Also, note that the mutual information is between the output and latent variables, rather than the parameters of the model. The key overarching contribution of latent-level sampling methods lies in the conditioning of generative models on the input image. This section briefly introduces Generative Adversarial Networks (Section 4.2.1), Variational Autoencoders (Section 4.2.2), and Denoising Diffusion Probabilistic Models (Section 4.2.3), and outlines how these architectures are commonly adapted for probabilistic segmentation.

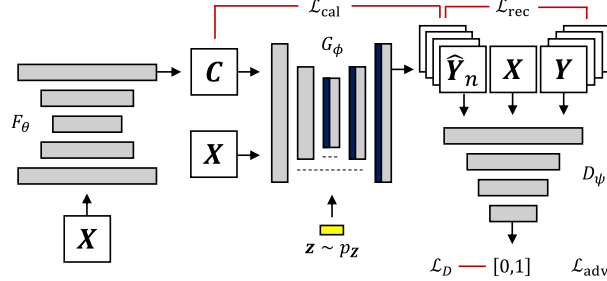


Figure 7: Diagram of the Calibrated Adversarial Refinement network Kassapis et al. (2021), based on the Generative Adversarial Network with additional loss terms.

4.2.1 Generative Adversarial Networks (GANs)

A straightforward approach is to simply learn the marginalization in Equation (12) through sampling from an unconditional prior density, $p_{\mathbf{z}} = \mathcal{N}(\mu = 0, \Sigma = \mathbf{I})$, and mapping this to segmentation Y through a *generator* $G_\phi : \mathcal{X} \times \mathcal{Z} \rightarrow \mathcal{Y}$. Goodfellow et al. (2014) show that this approach can be notably enhanced through the incorporation of a discriminative function (the *discriminator*), denoted as $D_\psi : \mathbb{R}^{C \times D} \rightarrow [0, 1]$. In this way, G_ϕ learns to reconstruct realistic images using the discriminative capabilities of D_ψ , making sufficient guidance from D_ψ to G_ϕ imperative. We can denote the cost of G_ϕ in the GAN as the negative cost of D_ψ as

$$J_{G_\phi} = -J_{D_\psi} = \mathbb{E}_{p_{\mathcal{D}}} [\log D_\psi(\mathbf{y})] - \mathbb{E}_{p_{\mathbf{z}}} \mathbb{E}_{p_{\mathcal{D}}} [\log(1 - D_\psi(G_\phi(\mathbf{z}, \mathbf{x})))]. \quad (14)$$

While conditional GANs have been used for semantic segmentation earlier (Isola et al., 2017), Kassapis et al. (2021) explicitly contextualized the architecture within aleatoric uncertainty quantification, using their proposed Calibrated Adversarial Refinement (CAR) network (see Figure 7). The calibration network, $F_\theta : \mathbb{R}^{C \times D} \rightarrow \mathbb{R}^{K \times D}$, initially provides a SoftMax activated prediction as $F_\theta(\mathbf{x}) = c$, with (cross-entropy) reconstruction loss

$$\mathcal{L}_{\text{rec}} = -\mathbb{E}_{p_{\mathcal{D}}} [\log p_\theta(\mathbf{c}|\mathbf{x})]. \quad (15)$$

Then, the conditional refinement network G_θ uses \mathbf{c} together with input image \mathbf{x} and latent samples $\mathbf{z}_i \sim p_{\mathbf{z}}$ injected at multiple decomposition scales i , to predict various segmentation maps. Furthermore, the refinement network is subject to the adversarial objective

$$\mathcal{L}_{\text{adv}} = -\mathbb{E}_{p_{\mathcal{D}}} \mathbb{E}_{p_{\mathbf{z}}} [\log D_\psi(G_\phi(F_\theta(\mathbf{x}), \mathbf{z}), \mathbf{x})], \quad (16)$$

which is argued to elicit superior structural qualities compared to relying solely on cross-entropy loss. At the same time, the discriminator opposes the optimization with

$$\mathcal{L}_D = -\mathbb{E}_{p_{\mathbf{z}}} \mathbb{E}_{p_{\mathcal{D}}} [1 - \log D_\psi(G_\phi(F_\theta(\mathbf{x}), \mathbf{z}), \mathbf{x})] - \mathbb{E}_{p_{\mathcal{D}}} [\log D_\psi(\mathbf{y})]. \quad (17)$$

Finally, the average of the N segmentation maps generated from G_ϕ are compared against the initial prediction of F_θ through the calibration loss, which is the analytical KL-divergence between the two categorical densities, denoted by

$$\mathcal{L}_{\text{cal}} = \mathbb{E}_{p_{\mathcal{D}}} \text{KL}[p_\phi(\mathbf{y}|\mathbf{c}, \mathbf{x}) \parallel p_\theta(\mathbf{c}|\mathbf{x})]. \quad (18)$$

In this way, the generator loss can be defined as

$$\mathcal{L}_G = \mathcal{L}_{\text{adv}} + \lambda \cdot \mathcal{L}_{\text{cal}}, \quad (19)$$

with hyperparameter $\lambda \geq 0$. The purpose of the calibration network is argued to be threefold. Namely, it (1) sets a calibration target for \mathcal{L}_{cal} , (2) provides an alternate representation of \mathbf{X} to G_ϕ , and (3) allows for sample-free aleatoric uncertainty quantification. The refinement network can be seen as modeling the spatial dependency across the pixels, which enables sampling coherent segmentation maps.

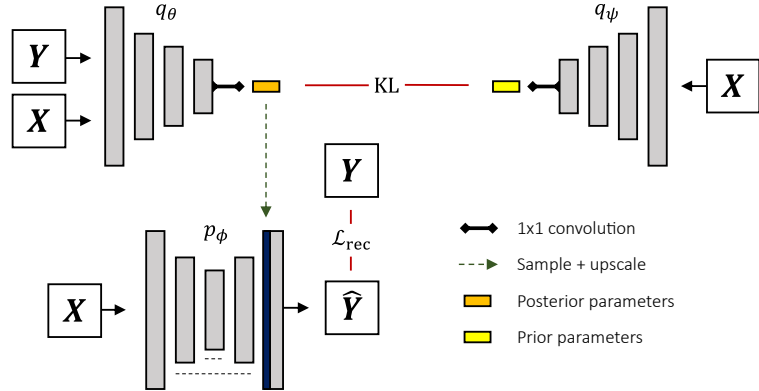


Figure 8: Depiction of the Probabilistic U-Net (Kohl et al., 2019b) based on a conditional Variational Autoencoder (Kingma & Welling, 2013). The latent samples are inserted at the final stages of a U-Net through a tiling operation.

4.2.2 Variational Autoencoders (VAEs)

Techniques such as GANs rely on implicit distributions and are void of any notion of data likelihoods. An alternative approach estimates the Bayesian posterior w.r.t. the latent variables, $p(\mathbf{Z}|\mathbf{Y}, \mathbf{X})$, with an approximation $q_\theta(\mathbf{Z}|\mathbf{Y}, \mathbf{X})$, obtained by maximizing the conditional Evidence Lower Bound (ELBO)

$$p(\mathbf{Y}|\mathbf{X}) = \log \int q_\theta(\mathbf{z}|\mathbf{Y}, \mathbf{X}) \frac{p(\mathbf{z}, \mathbf{Y}|\mathbf{X})}{q_\theta(\mathbf{z}|\mathbf{Y}, \mathbf{X})} d\mathbf{z} \quad (20a)$$

$$\geq \mathbb{E}_{q_\theta(\mathbf{z}|\mathbf{Y}, \mathbf{X})} \left[\frac{p(\mathbf{z}, \mathbf{Y}|\mathbf{X})}{q_\theta(\mathbf{z}|\mathbf{Y}, \mathbf{X})} \right] \quad (20b)$$

$$= \mathbb{E}_{q_\theta(\mathbf{z}|\mathbf{Y}, \mathbf{X})} [\log p_\phi(\mathbf{Y}|\mathbf{z}, \mathbf{X})] - \text{KL}[q_\theta(\mathbf{z}|\mathbf{Y}, \mathbf{X})||q_\psi(\mathbf{z}|\mathbf{X})], \quad (20c)$$

where Jensen’s inequality justifies moving the expectation outside the logarithm. The first term in Equation (20) represents the reconstruction cost of the decoder, subject to the latent code \mathbf{Z} and input image \mathbf{X} . The second term is the Kullback-Leibler (KL) divergence between the approximate posterior and prior density. As a consequence of the mean-field approximation, all involved densities are modeled by axis-aligned Gaussian densities and amortized through neural networks, parameterized by ϕ , θ and ψ . The predictive distribution after observing dataset \mathcal{D} is then obtained as

$$p(\mathbf{Y}|\mathbf{x}^*) = \int p_\phi(\mathbf{Y}|\mathbf{z}, \mathbf{x}^*) q_\theta(\mathbf{z}|\mathbf{x}^*) d\mathbf{z}. \quad (21)$$

The implementation of the conditional ELBO in Equation (20) can be achieved through the well known VAE architecture (Kingma & Welling, 2013). Furthermore, some additional design choices lead to the Probabilistic U-Net (PU-Net) (Kohl et al., 2019b). Firstly, the latent variable \mathbf{Z} is only introduced at the final layers of a U-Net conditioned on the images. The latent vector is up-scaled through tiling and then concatenated with the feature maps of the penultimate layer, which is followed by a sequence of 1×1 convolution for classification. When involving conditional latent variables in this manner, it is expected that most of the semantic feature extraction and delineation are performed in the U-Net, while the variability in the latent samples is almost exclusively related to the segmentation variability. Therefore, relatively smaller values of d are feasible than what is commonly used in conventional image generation tasks. Similar to related research on the VAE (Zhao et al., 2017; Bousquet et al., 2017; Higgins et al., 2017; Van Den Oord et al., 2017; Rezende & Mohamed, 2015), much work has been dedicated to improving the PU-Net.

Density reparameterization Augmenting a Normalizing Flow (NF) to the posterior density of a VAE is a commonly used tactic to improve its expressiveness (Rezende & Mohamed, 2015). This phenomenon has

also been successfully applied to VAE-like models such as the PU-Net (Valiuddin et al., 2021; Selvan et al., 2020). NFs are a class of generative models that utilize k consecutive bijective transformations $f_k : \mathbb{R}^D \rightarrow \mathbb{R}^D$ as $f = f_K \circ \dots \circ f_k \circ \dots \circ f_1$, to express exact log-likelihoods of arbitrarily complex approximations of the posterior $p(\mathbf{z}|\mathbf{x})$, where symbol \circ indicates functional composition. The approximated posteriors in turn induce an approximate of $p(\mathbf{x}|\mathbf{z}) = p(\mathbf{z}|\mathbf{x}) \frac{p(\mathbf{x})}{p(\mathbf{z})}$ and are often denoted as $\log p(\mathbf{x})$ for simplicity. The fractional term accounts for the change in probability space and corresponds to the log-Jacobian determinant, as given by the Change of Variables theorem. Thus, we can denote

$$\log p(\mathbf{x}) = \log p_{\mathbf{z}}(\mathbf{z}_0) - \sum_{k=1}^K \log \left| \det \frac{df_k(\mathbf{z}_{k-1})}{d\mathbf{z}_{k-1}} \right|, \quad (22)$$

where \mathbf{z}_k and \mathbf{z}_{k-1} are intermediate variables from intermediate densities and $\mathbf{z}_0 = \mathbf{f}^{-1}(\mathbf{x})$. Equation (22) can be substituted in the conditional ELBO objective in Equation (20) to obtain

$$\begin{aligned} p(\mathbf{Y}|\mathbf{X}) &\geq \mathbb{E}_{q_{\theta}(\mathbf{z}|\mathbf{Y}, \mathbf{X})} [\log p_{\phi}(\mathbf{Y}|\mathbf{z}, \mathbf{X})] \\ &\quad - \text{KL}[q_{\theta}(\mathbf{z}_0|\mathbf{Y}, \mathbf{X}) || q_{\psi}(\mathbf{z}_k|\mathbf{X})] - \mathbb{E}_{q_{\theta}(\mathbf{z}_0|\mathbf{Y}, \mathbf{X})} \left[\sum_{k=1}^K \log \left| \det \frac{df_k(\mathbf{z}_{k-1})}{d\mathbf{z}_{k-1}} \right| \right], \end{aligned} \quad (23)$$

where the objective consists of a reconstruction term, sample-based KL-divergence and a likelihood correction term for the change in probability density induced by the NF. Bhat et al. (2023; 2022a) compare this approach with other parameterizations of the latent space, including a mixture of Gaussians and low-rank approximation of the full covariance matrix. Valiuddin et al. (2024b) show that the latent space can converge to contain non-informative latent dimensions, undermining the capabilities of the latent-variable approach, generally referred to as mode or posterior collapse (Chen et al., 2016; Zhao et al., 2017). Their proposition considers the alternative formulation of the ELBO, specified as

$$\begin{aligned} \log p(\mathbf{Y}|\mathbf{X}) &\geq \mathbb{E}_{q_{\theta}(\mathbf{z}|\mathbf{Y}, \mathbf{X})} [\log p_{\phi}(\mathbf{Y}|\mathbf{X}, \mathbf{z})] \\ &\quad - \text{KL}[q_{\theta}(\mathbf{z}|\mathbf{X}) || q_{\psi}(\mathbf{z}|\mathbf{X})] - I(\mathbf{Y}, \mathbf{Z}|\mathbf{X}). \end{aligned} \quad (24)$$

The proposed novel objective maximizes the contribution of the (expected) mutual information between latent and output variables, i.e. the aleatoric uncertainty term of the predictive entropy in Equation (13). This enables the introduction of the updated objective

$$\begin{aligned} \mathcal{L} &= -\mathbb{E}_{q_{\theta}(\mathbf{z}|\mathbf{Y}, \mathbf{X})} [\log p_{\phi}(\mathbf{Y}|\mathbf{X}, \mathbf{z})] \\ &\quad + \alpha \cdot \text{KL}[q_{\theta}(\mathbf{z}|\mathbf{Y}, \mathbf{X}) || p_{\psi}(\mathbf{z}|\mathbf{X})] + \beta \cdot S_{\epsilon}[q_{\theta}(\mathbf{z}|\mathbf{X}) || p_{\psi}(\mathbf{z}|\mathbf{X})], \end{aligned} \quad (25)$$

with S_{ϵ} being the Sinkhorn divergence Cuturi (2013) and α, β denoting hyperparameters. This adaptation results in a more uniform latent space leading to increased model performance. Also, modeling the ELBO of the joint density has been explored (Zhang et al., 2022b). This formulation results in an additional reconstruction term and forces the latent variables to be more congruent with the data. Furthermore, constraining the latent space to be discrete has resulted in some improvements, where it is hypothesized that this partially addresses the model collapse phenomenon (Qiu & Lui, 2020).

Multi-scale approach Learning latent features over several hierarchical scales can provide expressive densities and interpretable features across various abstraction levels (Sønderby et al., 2016; Kingma et al., 2016; Klushyn et al., 2019; Gregor et al., 2015; Ranganath et al., 2016). Such models are commonly categorized under hierarchical VAE (HVAE) modeling. Often, an additional Markov assumption of length T is placed on the posterior as

$$q_{\theta}(\mathbf{Z}_{1:T}|\mathbf{Y}, \mathbf{X}) = q_{\theta}(\mathbf{Z}_1|\mathbf{Y}, \mathbf{X}) \prod_{t=2}^T q_{\theta}(\mathbf{Z}_t|\mathbf{Z}_{t-1}). \quad (26)$$

Consequently, the conditional ELBO is denoted as

$$\begin{aligned} p(\mathbf{Y}|\mathbf{X}) &\geq \mathbb{E}_{q_{\theta}(\mathbf{z}|\mathbf{Y}, \mathbf{X})} [\log p_{\phi}(\mathbf{Y}|\mathbf{z}, \mathbf{X})] \\ &\quad - \sum_{t=2}^T \text{KL}[q_{\theta}(\mathbf{z}_t|\mathbf{Y}, \mathbf{X}, \mathbf{z}_{1:t-1}) || q_{\psi}(\mathbf{z}_t|\mathbf{z}_{1:t-1})] - \text{KL}[q_{\theta}(\mathbf{z}_1|\mathbf{Y}, \mathbf{X}) || q_{\psi}(\mathbf{z}_1|\mathbf{X})]. \end{aligned} \quad (27)$$

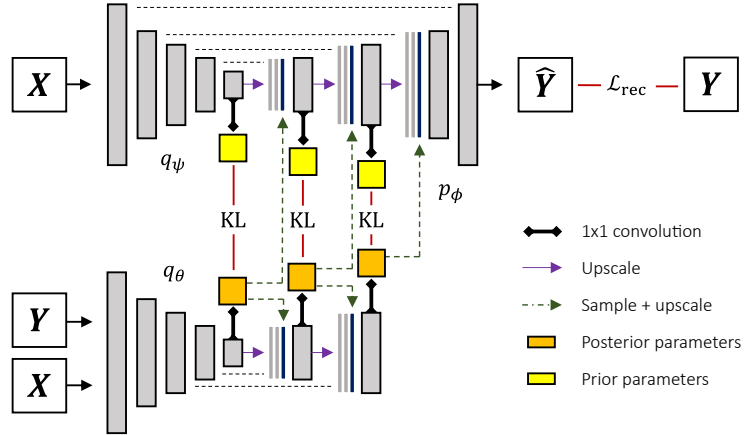


Figure 9: Hierarchical Probabilistic U-Net (Kohl et al., 2019a) based on a hierarchical Variational Autoencoder (Kingma & Welling, 2013; Sønderby et al., 2016; Klushyn et al., 2019). Instead of a single latent code, multiple decomposition scales encode the segmentation variability, depending on the depth of the U-Net structure.

This objective is implemented in the Hierarchical PU-Net (Kohl et al., 2019a) (HPU-Net, depicted in Figure 9), which learns a latent representation at multiple decomposition levels of the U-Net. Residual connections in the convolutional layers are necessary to prevent degeneracy of uninformative latent variables with the KL divergence rapidly approaching zero. For similar reasons, the Generalized ELBO with Constrained Optimization (GECO) objective is employed, which extends Equation (27) to

$$\begin{aligned} \mathcal{L}_{\text{GECO}} = & \lambda \cdot (\mathbb{E}_{q_\theta(\mathbf{z}|\mathbf{Y}, \mathbf{X})}[\log p_\phi(\mathbf{Y}|\mathbf{z}, \mathbf{X})] - \kappa) \\ & - \sum_{t=2}^T \text{KL}[q_\theta(\mathbf{z}_t|\mathbf{Y}, \mathbf{X}, \mathbf{z}_{1:t-1}) \parallel q_\psi(\mathbf{z}_t|\mathbf{z}_{1:t-1})] - \text{KL}[q_\theta(\mathbf{z}_1|\mathbf{Y}, \mathbf{X}) \parallel q_\psi(\mathbf{z}_1|\mathbf{X})]. \end{aligned} \quad (28)$$

Hyperparameter λ is the Lagrange multiplier update through the Exponential Moving Average of the reconstruction, which is constrained to reach target value κ , empirically set beforehand to an appropriate value. Finally, online negative hard mining is used to only backpropagate 2% of the worst performing pixels, which are stochastically picked with the Gumbel-SoftMax trick (Jang et al., 2016; Huijben et al., 2022). Furthermore, PHiSeg (Baumgartner et al., 2019) takes a similar approach to the HPU-Net. However, PHiSeg places residual connections between latent vectors across decompositions rather than in the convolutional layers. Furthermore, *deep supervision* at each decomposition scale to enforce the disentanglement between latent variables.

Extension to 3D Early methods for uncertainty quantification in medical imaging primarily utilized 2D slices from three-dimensional (3D) datasets, leading to a potential loss of critical spatial information and subtle nuances often necessary for accurate delineation. This limitation has spurred research into 3D probabilistic segmentation techniques with ELBO-based models, aiming to preserve the integrity of entire 3D structures. Initial works (Chotzoglou & Kainz, 2019; Long et al., 2021a) demonstrate that the PU-Net can be adapted by replacing all 2D operations with their 3D variants. Crucially, the fusion of the latent sample with 3D extracted features is achieved through a 3D tiling operation. Viviers et al. (2023c) additionally augment a Normalizing Flow to the posterior density for improved expressiveness, as discussed in Section 4.2.2. Further enhancements to the architecture include the implementation of the 3D HPU-Net (Saha et al., 2020), an updated feature network incorporating the attention mechanisms, a nested decoder, and different reconstruction loss components tailored to specific applications (Saha et al., 2021a).

Conditioning on annotator It can be relevant to model the annotators independently in cases with consistent annotator-segmentation pairs in the dataset. This can be achieved by conditioning the learned densities on the annotator itself (Gao et al., 2022; Schmidt et al., 2023). For example, features of a U-Net can be combined with samples from annotator-specific Gaussian-distributed posteriors (Schmidt et al.,

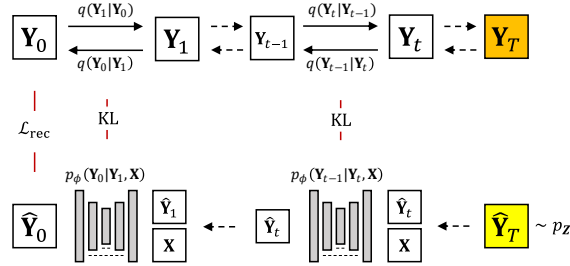


Figure 10: Illustration of the Diffusion Probabilistic Models (Ho et al., 2020). The model learns to remove noise that has been gradually added to the input image.

2023). Considering the approach from Gao et al. (2022), generating a segmentation mask is achieved by first sampling an annotator from a categorical prior distribution $\mathcal{C}(\pi_k(\mathbf{x}))$, governed by the image conditional parameters $\pi_k(\mathbf{x})$ for the k -th annotator. Then, samples are taken from its corresponding prior density as $\mathbf{z}_k \sim p_k(\mathbf{z}_k)$ to reconstruct a segmentation through an image-conditional decoder $y = F(\mathbf{x}, \mathbf{z}_k)$. The parameters $\pi_k(\mathbf{z}_k)$ can also be used to weigh the corresponding predictions to express the uncertainty in the prediction ensemble. Additionally, consistency between the model and ground-truth distribution is enforced through an optimal transport loss between the set of predictions and labels.

4.2.3 Denoising Diffusion Probabilistic Models (DDPMs)

Recent developments in generative modeling have resulted in a family of models known as Denoising Diffusion Probabilistic Models (Ho et al., 2020; Song et al., 2022; 2020). Such models are especially renowned for their expressive power by being able to encapsulate large and diverse datasets. While several perspectives can be used to introduce the DDPMs, we build upon the earlier discussed HVAE (Section 4.2.2) to maintain cohesiveness with the overall manuscript. Specifically, we describe three additional modifications to the HVAE (Luo, 2022). Firstly, the latent dimensionality is set equal to the spatial data dimensions, i.e. $d = D$. As a consequence, redundant notation of \mathbf{Z} is removed and \mathbf{Y} is instead subscripted with $t \in \{1, \dots, T\}$, indicating the encoding depth, where \mathbf{Y}_0 is the initial segmentation mask. Secondly, the encoding process (or *forward process*) is predefined as a linear Gaussian model such that

$$q(\mathbf{Y}_T | \mathbf{Y}_0) = p(\mathbf{Y}_0) \prod_{t=1}^T q(\mathbf{Y}_t | \mathbf{Y}_{t-1}), \quad (29)$$

where

$$q(\mathbf{y}_t | \mathbf{Y}_{t-1}) = \mathcal{N}(\mathbf{y}_t; \boldsymbol{\mu} = \sqrt{\alpha_t} \mathbf{Y}_{t-1}, \boldsymbol{\Sigma} = (1 - \alpha_t) \cdot \mathbf{I}), \quad (30)$$

with noise schedule $\boldsymbol{\alpha} = \{\alpha_t\}_{t=1}^T$. Then, the decoding or *reverse process* can be learned through $p_\phi(\mathbf{Y}_{t-1} | \mathbf{Y}_t, \mathbf{x})$. The ELBO for this objective is defined as

$$\begin{aligned} p(\mathbf{Y} | \mathbf{X}) &\geq \mathbb{E}_{q(\mathbf{Y}_1 | \mathbf{Y}_0)} [\log p_\phi(\mathbf{Y}_0 | \mathbf{y}_1, \mathbf{X})] \\ &\quad + \sum_{t=2}^T \mathbb{E}_{q(\mathbf{Y}_t | \mathbf{Y}_0)} [\text{KL}[q(\mathbf{y}_{t-1} | \mathbf{y}_t) || p_\phi(\mathbf{y}_{t-1} | \mathbf{y}_t, \mathbf{X})]] + \underbrace{\mathbb{E}_{q(\mathbf{Y}_T | \mathbf{Y}_0)} \left[\log \frac{p(\mathbf{y}_T)}{q(\mathbf{y}_T | \mathbf{Y}_0)} \right]}_{\approx 0}. \end{aligned} \quad (31)$$

As denoted, the regularization term is assumed to be zero, since it is assumed that a sufficient amount of steps T are taken such that $q(\mathbf{y}_T | \mathbf{y}_0)$ is approximately normally distributed. With the reparameterization trick (Kingma & Welling, 2013), the forward process is governed by random variable $\epsilon \sim \mathcal{N}(0, 1)$. As such, the KL divergence in the second term can be interpreted as predicting \mathbf{Y}_0 , the source noise ϵ or the score $\nabla_{\mathbf{Y}_t} \log q(\mathbf{y}_t)$ (gradient of the data log-likelihood) from \mathbf{Y}_t , depending on the parameterization. This is in almost all instances approximated with a U-Net (Ronneberger et al., 2015).

The proposed methodologies for segmentation vary in the conditioning of the reverse process on the input image (Wolleb et al., 2021; Wu et al., 2023b;a; Amit et al., 2021). For instance, Wolleb et al. (2021)

concatenate the input image with the noised segmentation mask. Wu et al. (2023b) insert encoded image features to the U-Net bottleneck. Additionally, information on predictions Y_t at a time step t is provided in the intermediate layers of the conditioning encoder. This is performed by applying the Fast Fourier Transform (FFT) on the U-Net encoding, followed by a learnable attention map and the inverse FFT. The procedure of applying attention on the spectral domain of the U-Net encoding has also been implemented with transformers in follow-up work (Wu et al., 2023a). Segdiff (Amit et al., 2021) also encode both current time step and input image, but combine the extracted features by simple summation prior to inferring it through the U-Net. It has also been proposed to model Bernoulli instead of Gaussian noise (Chen et al., 2023a; Zbinden et al., 2023; Rahman et al., 2023; Bogensperger et al., 2023).

5 Parameter modeling

The key distinction between epistemic and aleatoric uncertainty lies in their origins: epistemic uncertainty arises from model ignorance (i.e. related to the parameters), whereas aleatoric uncertainty reflects inherent statistical variability in the data. Consequently, unlike aleatoric uncertainty, epistemic uncertainty should not only be quantified but ideally also minimized. Epistemic uncertainty can be further categorized into two distinct types (Hüllermeier & Waegeman, 2021). The first type pertains uncertainty related to the capacity of the model. For example, under-parameterized models or approximate model posteriors, that can become too stringent to appropriately resemble the true posterior. The ambiguity on the best parameters given the limited capacity induces uncertainty in the learning process, which is also known as *model uncertainty*. Nevertheless, given the complexity of contemporary parameter-intensive CNNs, the model uncertainty is often assumed to be negligible. A more significant contribution to the epistemic uncertainty is due to the limited data availability, known as *approximation uncertainty*, and can often be reduced by collecting more data.

As discussed in Section 3, epistemic uncertainty is captured by modeling the posterior distribution defined in Equation (1). However, evaluating the true Bayesian posterior is impeded by the intractability of the data likelihood in the denominator. Hence, extensive efforts have been taken to obtain viable approximations, such as using Mean-Field Variational Inference Blundell et al. (2015), Markov Chain Monte Carlo (MCMC) Neal (2012), Monte-Carlo Dropout Gal & Ghahramani (2016); Kingma et al. (2015), Model Ensembling Lakshminarayanan et al. (2017), Laplace approximations Mackay (1992), Stochastic Gradient MCMCs Korattikara Balan et al. (2015); Springenberg et al. (2016); Welling & Teh (2011), assumed density filtering Hernández-Lobato & Adams (2015) and expectation propagation Hensel clever et al. (2017); Louizos & Welling (2016). We refer to any neural network that approximates the Bayesian posterior over model parameters as a Bayesian Neural Network (BNN). Unlike modeling the output distribution directly, sampling parameters from the posterior naturally induces spatial coherence in the output. As a result, existing methods are often simple extensions of conventional classification BNNs, rather than leveraging techniques tailored for segmentation tasks. This section discusses three methods for modeling epistemic uncertainty. The most commonly used approach is Variational Inference (VI) over model parameters (Section 5.1). Test-time augmentation, often mistakenly regarded as an aleatoric method, is addressed in Section 5.3. Finally, Laplace Approximations are examined in Section 5.2.

5.1 Variational Inference

Consider a simpler, tractable density $q(\boldsymbol{\theta}|\boldsymbol{\eta})$, parameterized by $\boldsymbol{\eta}$ (e.g. a gaussian with $\boldsymbol{\eta} = \{\mu, \sigma\}$), to approximate posterior $p(\boldsymbol{\theta}|\mathbf{y}, \mathbf{x})$. Then, we can employ Variational Inference (VI) w.r.t. to the parameters, by minimizing the Kullback-Leibler (KL) divergence between the true and approximated Bayesian posterior as

$$\begin{aligned}
 \boldsymbol{\eta}^* &= \arg \min_{\boldsymbol{\theta}} \text{KL} [q(\boldsymbol{\theta}|\boldsymbol{\eta}) \parallel p(\boldsymbol{\theta}|\mathcal{D})] \\
 &= \arg \min_{\boldsymbol{\theta}} \int q(\boldsymbol{\theta}|\boldsymbol{\eta}) \log \frac{q(\boldsymbol{\theta}|\boldsymbol{\eta})}{p(\mathbf{Y}|\mathbf{x}, \boldsymbol{\theta})p(\mathbf{x}, \boldsymbol{\theta})} d\boldsymbol{\theta} \\
 &= \arg \min_{\boldsymbol{\theta}} \text{KL} [q(\boldsymbol{\theta}|\boldsymbol{\eta}) \parallel p(\boldsymbol{\theta})] - \mathbb{E}_{q(\boldsymbol{\theta}|\boldsymbol{\eta})} [\log p(\mathbf{y}|\mathbf{x}, \boldsymbol{\theta})],
 \end{aligned} \tag{32}$$

where the parameter-independent terms are constant and therefore excluded from notation. In the case of a deterministic encoder, i.e. $q(\boldsymbol{\theta}|\boldsymbol{\eta}) = \delta(\boldsymbol{\theta} - \boldsymbol{\theta}^*)$, the formulation collapses to the MAP estimate in Equation (5). A popular choice for the approximated variational posterior is the Gaussian distribution, i.e. a mean μ and covariance σ parameter for each element of the convolutional kernel, usually with zero-mean unitary Gaussian prior densities. However, the priors can be also learned through Empirical Bayes (Bishop, 1995). Furthermore, backpropagation is possible with the *reparameterization trick* (Kingma & Welling, 2013) and within this context, the procedure is referred to as Bayes by Backprop (BBB) (Blundell et al., 2015) and has later been improved with the Local Reparameterization trick (Kingma et al., 2015). In addition to approximating the posterior, sampling from it yields multiple parameter permutations, effectively enriching the model’s hypothesis space, a phenomenon also referred to as model combination (Minka, 2000; Clarke, 2003; Lakshminarayanan, 2016). In most cases, VI is not performed explicitly. Instead, simpler techniques are employed, with the resulting parameter permutations hypothesized to serve as a proxy. We discuss two such methods: Monte Carlo Dropout (Section 5.1.1) and Ensembling (Section 5.1.2). See Figure 11 for an illustration of each method. All of these methods have been widely applied to segmentation. However, unlike aleatoric uncertainty modeling, their implementations are often more generic and not specifically tailored to segmentation tasks. Therefore, we provide only a brief overview here, followed by a more in-depth discussion in later sections related to various applications.

5.1.1 Monte Carlo Dropout

Dropout is a common technique used to regularize neural networks (Wager et al., 2013) by randomly “switching off” nodes of the neural network. Using Dropout can also be interpreted as a first-order equivalent L_2 regularization with additionally transforming the input with the inverse diagonal Fisher information matrix (Wager et al., 2013). Furthermore, with *Monte-Carlo Dropout* (MC Dropout), the random node switching is continued during test time, effectively sampling new sets of parameters, mimicking samples from an implicit parameter distribution $q(\tilde{\boldsymbol{\theta}}|\boldsymbol{\theta}, p)$, defined as

$$\mathbf{n} \sim \text{Bernoulli}(p), \quad (33a)$$

$$\tilde{\boldsymbol{\theta}} = \boldsymbol{\theta} \odot \mathbf{n}, \quad (33b)$$

with probability p and vector \mathbf{n} operating element-wise on the parameters. It has been shown that MC Dropout can be interpreted as approximate VI in a Deep Gaussian Process (Gal & Ghahramani, 2016). In this manner, such a method is able to provide multimodal estimates of the model uncertainty. As noted by Gal et al. (2017a), the variance in the model output is primarily governed by the magnitudes of the weights rather than the dropout rate p . The dropout rate is usually optimized through grid search or simply set to $p = 0.5$. The relationship between p and the magnitude of the model weights has also been exploited to probabilistically prune neural networks Gonzalez-Carabarin et al. (2022). Gal et al. (2017a) propose to additionally learn p using gradient-based methods, known as Concrete Dropout, to increase the influence of p . As the name suggests, a continuous approximation to the discrete distribution is used, known as the Concrete distribution (Maddison et al., 2016; Jang et al., 2016), to enable path-wise derivatives through p . Also, a generalization of MC dropout has been proposed, where the weights of the network, rather than its hidden output, are set to zero (Mobiny et al., 2021).

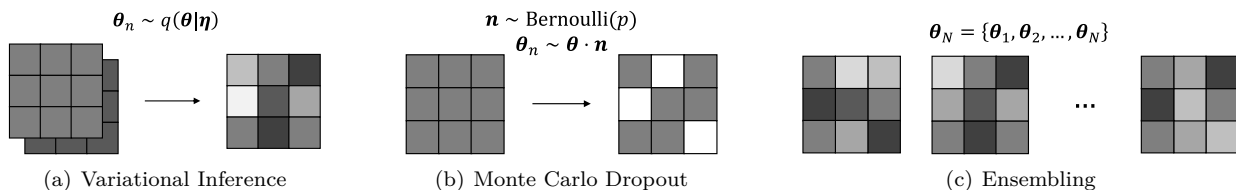


Figure 11: Three types of techniques are visualized to sample parameters of the convolutional kernels, (a) an approximation of the parameter density can be made, (b) taking samples can be mimicked with dropout during test time, or, (c) an ensemble of N different configurations can be explicitly modeled.

5.1.2 Ensembling

As mentioned earlier, MC dropout effectively optimizes over a set of sparse neural networks. From this perspective, explicitly ensembling multiple models can also be considered as an approximation of VI (Lakshminarayanan et al., 2017). To this end, we define the set of functions $\mathbf{f} = \{f_\theta^n\}_{n=1}^M$, with M representing the number of models in the ensemble. Then, it is relatively simple to obtain $\Theta = \{\theta_m\}_{m=1}^M$, which can be interpreted as samples from an approximate posterior. Ensembling in only the latter parts of a neural network (typically the decoder) is referred to as M-heads, i.e. the network has multiple outputs. Often, the M obtained parameters are from M separate training sessions. However, it has also been proven effective to ensemble from a single training session, by saving the parameters at multiple stages or training with different weight initializations (Dahal et al., 2020; Xie et al., 2013; Huang et al., 2017). A closely related concept to ensembling is known as Mixture of Experts (MoE), where each model in the ensemble (an ‘expert’) is trained on specific subsets of the data (Jacobs et al., 1991). In such settings, however, a gating mechanism is usually applied after combining the expert hypotheses.

5.2 Laplace approximation

It can be shown that the intractable posterior in Equation (2) can be estimated as

$$\begin{aligned} p(\theta|\mathcal{D}) &\approx \frac{(\det \mathbf{H})^{\frac{1}{2}}}{(2\pi)^{\frac{d}{2}}} \exp\left(-\frac{1}{2}(\theta - \theta_{\text{MAP}})^T \mathbf{H}(\theta - \theta_{\text{MAP}})\right) \\ &= \mathcal{N}(\theta|\mu = \theta_{\text{MAP}}, \Sigma = \mathbf{H}^{-1}), \end{aligned} \quad (34)$$

with θ_{MAP} being the Maximum a Posteriori solution and Hessian matrix $\mathbf{H} = -\nabla^2 \log h(\theta)|_{\theta_{\text{MAP}}}$, i.e. the second derivative of the loss function evaluated at θ_{MAP} . This approach, known as the Laplace Approximation (LA) (Laplace, 1774), has the merit that it can be performed *post-hoc* to e.g. pretrained neural networks. However, estimating the Hessian can become infeasible, as computation scales quadratically with the model parameters. This is usually circumvented by treating neural network partly probabilistic and/or approximating the Hessian with a more simplified matrix structure (Martens & Grosse, 2015; Botev et al., 2017; Daxberger et al., 2021).

5.3 Test-time augmentation

An image \mathbf{X} can be understood as a one-of-many visual representations of the object of interest. For example, systematic noise, translation or rotation result in many realistic variations that approximately retain image semantics. Hence, data augmentation (Krizhevsky et al., 2012) has been used at test time (explaining the name test-time augmentation, or TTA), argued to obtain uncertainty estimates by efficiently exploring the locality of the likelihood function (Ayhan & Berens, 2022). By randomly augmenting input images with invertible transformation $\tilde{\mathbf{x}} = T_\zeta(\mathbf{x})$, with transformation parameters ζ , a prediction is obtained with $\tilde{\mathbf{y}} = f_\theta(\tilde{\mathbf{x}})$ and can then be inverted through $\mathbf{y} = T_\zeta^{-1}(\tilde{\mathbf{y}})$. Repeatedly performing this procedure results in a set of segmentation masks, which serve as an estimate of $p(\mathbf{Y}|\mathbf{X}, \theta)$. In segmentation literature, it has been hypothesized that TTA encapsulates the aleatoric uncertainty in a better way (Wang et al., 2019a; Ayhan & Berens, 2022; Zhang et al., 2022a; Wang et al., 2019b; Rakic et al., 2024; Whitbread & Jenkinson, 2022; Roshanzamir et al., 2023). However, literature opposing this also exist and even suggests that TTA enables the modeling of epistemic uncertainty (Hu et al., 2022). Kahl et al. (2024) draw parallels with BNNs and demonstrate this through the (by now) familiar decomposition of the predictive uncertainty

$$H[\mathbf{Y}|\mathbf{x}, \theta] = \underbrace{I[\mathbf{Y}, \mathbf{t}|\mathbf{x}, \theta]}_{\text{epistemic}} + \overbrace{\mathbb{E}_{\mathbf{t}}[H[\mathbf{Y}|\mathbf{t}, \mathbf{x}, \theta]]}^{\text{aleatoric}}. \quad (35)$$

where t are sampled augmentations from the input space \mathcal{T} . Aleatoric uncertainty is captured because a perfectly trained model produces consistent predictions across augmentations of known data. Epistemic uncertainty arises when the mutual information between the predicted label and augmentation is greater than zero for unseen data, indicating the model has not yet learned invariance for such inputs.

6 Applications

This section briefly provides literature that incorporates uncertainty into downstream tasks using segmentation models. These tasks can be broadly categorized into four main groups: estimating the segmentation mask distribution subject to observer variability (Section 6.1), reducing labeling costs using Active Learning (Section 6.2), model introspection (i.e. ability to self-assess Section 6.3) and improved generalization (Section 6.4). For quick reference, Table 5 summarizes the types of dataset domains (e.g., medical, outdoor scenes) associated with various downstream tasks.

6.1 Observer variability

After observing sufficient data, the variability in the predictive distribution is often considered to be negligible and is therefore omitted. Nevertheless, this assumption becomes excessively strong in ambiguous modalities, where its consequence is often apparent with multiple varying, yet plausible annotations for a single image. Additionally, such annotations can also vary due to differences in expertise and experience of annotators. The phenomenon of inconsistent labels across annotators is known as the *inter-observer* variability, while variations from a single annotator are referred to as the *intra-observer* variability (see Figure 12).

Annotators are models To contextualize this phenomenon within the framework of uncertainty quantification, annotators can be regarded as models themselves. For example, consider K separate annotators modeled through parameters ϕ_k with $k = 1, 2, \dots, K$. For a simple segmentation task, it can be expected that $\text{Var}[p(\phi_k)] \rightarrow 0$. In other words, each annotator is consistent in his delineation and the *intra-observer* variability is low. For cases with consensus across experts, i.e. yielding negligible inter-observer variability, the marginal approaches to $\text{Var}[p(\phi)] \rightarrow 0$. Asserting these two assumptions, it is valid to simply consider a point estimate of the posterior. Yet, this is rarely the case in many real-life applications and, as such, explicitly modeling the involved distributions becomes necessary.

Evaluation For evaluation, a commonly used metric minimizes the squared distance between arbitrary mean embeddings of the ground truth and predicted annotations using the kernel trick (Shawe-Taylor, 2004). This metric is known as Maximum Mean Discrepancy (MMD) or the Generalized Energy Distance (GED) (Gretton et al., 2012), denoted as

$$\text{GED}(P_Y, P_{\hat{Y}}) = \mathbb{E}_{\mathbf{y}, \mathbf{y}' \sim P_Y} [k(\mathbf{y}, \mathbf{y}')] + \mathbb{E}_{\hat{\mathbf{y}}, \hat{\mathbf{y}}' \sim P_{\hat{Y}}} [k(\hat{\mathbf{y}}, \hat{\mathbf{y}}')] - 2 \cdot \mathbb{E}_{\mathbf{y} \sim P_Y} \mathbb{E}_{\hat{\mathbf{y}} \sim P_{\hat{Y}}} [k(\mathbf{y}, \hat{\mathbf{y}})], \quad (36)$$

with marginals P_Y and $P_{\hat{Y}}$, representing the true and predictive segmentation distribution, and a distance represented by kernel $k : \mathcal{Y} \times \mathcal{Y} \rightarrow \mathbb{R}$, usually the (1–IoU) or (1–Dice) score (squared by the GED). However,

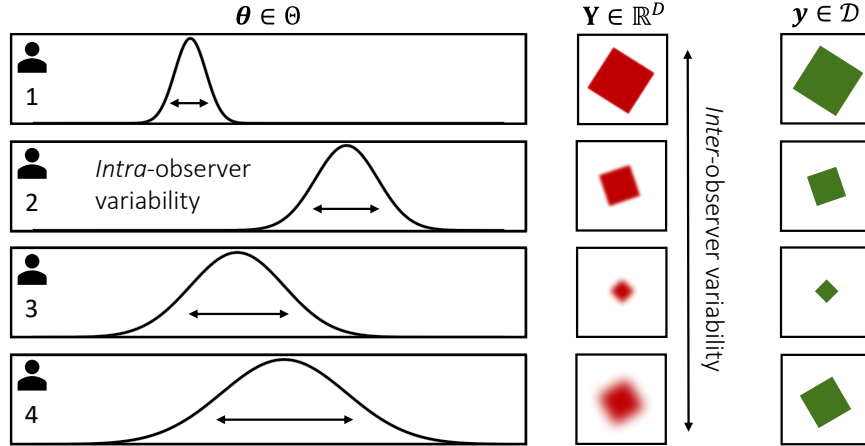


Figure 12: Visualization of the intra-observer variability in parameter space (left) and the inter-observer variability in data space (right).

Table 1: Methods used for the application of encapsulating Observer Variability.

Method	Literature
PixelCNN	Zhang et al. (2022c)
SSN	Monteiro et al. (2020); Kahl et al. (2024); Zepf et al. (2024; 2023a); Philps et al. (2024)
GAN	Kassapis et al. (2021)
VAE	Gao et al. (2022); Kohl et al. (2019b); Valiuddin et al. (2021); Selvan et al. (2020); Bhat et al. (2023; 2022a); Valiuddin et al. (2024b); Qiu & Lui (2020); Valiuddin et al. (2024a); Viviers et al. (2023c); Schmidt et al. (2023); Long et al. (2021b); Zepf et al. (2023a; 2024); Hu et al. (2022); Viviers et al. (2023b); Savadikar et al. (2021); Philps et al. (2024)
HVAE	Zhang et al. (2022b); Rafael-Palou et al. (2021); Kohl et al. (2019a); Baumgartner et al. (2019); Gantenbein et al. (2020)
DDPM	Chen et al. (2023a); Zbinden et al. (2023); Rahman et al. (2023)
MC dropout	Kahl et al. (2024); Philps et al. (2024)
Ensembling	Zepf et al. (2024); Hu et al. (2023)
TTA	Kahl et al. (2024)

solely relying on the GED has been criticized due to undesirable inductive biases Kohl et al. (2019a); Zepf et al. (2024). Hence, Kohl et al. (2019a) introduce an alternative metric known as Hungarian Matching (HM), which compares the predictions against the ground-truth labels through a cost matrix. This can be also formally denoted as finding the permutation matrix P , subject to the objective

$$\text{HM}(\mathcal{Y}, \hat{\mathcal{Y}}) = \frac{1}{N^2} \min_{\mathbf{P}} \text{Tr}(\mathbf{PM}), \quad (37)$$

where the elements of M are $M_{i,j} = k(\mathcal{Y}_i, \hat{\mathcal{Y}}_j)$, and N^2 represents the number of elements within the matrix. Subsequently, the unique optimal coupling between the two sets that minimize the average cost is determined through a combinatorial optimization algorithm. Hu et al. (2022) use the Normalized Cross Correlation (NCC) to measure the similarity between the true and predictive set, which can formally be defined as

$$\text{NCC} = \frac{1}{n\sigma\hat{\sigma}} \sum_i (a_i - \mu) \cdot (\hat{b}_i - \hat{\mu}), \quad (38)$$

with n being the number of pixels, and μ, σ and $\hat{\mu}, \hat{\sigma}$ the mean and standard deviation of the true and predicted segmentations set, respectively. Variables a and b represent the uncertainty map calculated through the pixel-wise variance across the true and predicted segmentations, respectively.

Approaches The most straightforward approach is to directly model the empirical stochasticity in the annotations with models that target the aleatoric uncertainty. Given that annotators have an intrinsically associated expertise, it can also be possible to model the annotator distribution. However, relying on the model to infer ambiguity in the parameters by observing the data, can become quite burdensome. This observation is reflected in literature, where we see that most approaches use conditional generative models to encapsulate observer variability (See Table 1). While conditional generative models have been successfully applied for the task at hand, it has been shown that such models, without explicit conditioning, do not encapsulate more subtle variations such as distinct labeling styles of annotators Zepf et al. (2023a). VAE-based Probabilistic U-Net is the most popular approached followed by its hierarchical variants (HPU-Net and PHI-Seg) and SSNs. More recently, the growing popularity of DDPMs is apparent in the field.

6.2 Active Learning

The field of active learning (Settles, 2009; Ren et al., 2021) aims to reduce the costly annotation procedure by careful selection of the most informative samples for training (Settles, 2009). In this way, the required labeled data is minimized and training convergence can be accelerated due to reduced redundancy. Active Learning

Table 2: Methods used for the application of Active Learning

Method	Literature
SoftMax	Kasarla et al. (2019); García Rodríguez et al. (2020); Xie et al. (2022); Wu et al. (2021); Burmeister et al. (2022); Gaillochet et al. (2023)
SSN	Kahl et al. (2024)
Adversarial VAE / GAN	Mahapatra et al. (2018); Kim et al. (2021); Sinha et al. (2019)
Ensembling	Yang et al. (2017); Nath et al. (2020); Khalili et al. (2024)
MC dropout	Kahl et al. (2024); Gorriz et al. (2017); Ozdemir et al. (2021); Hiasa et al. (2019); Li & Alstrøm (2020); Shen et al. (2021); Ma et al. (2024b); Gaillochet et al. (2023); Siddiqui et al. (2020); Sadafi et al. (2019)
TTA	Gaillochet et al. (2023)

is an extensively researched topic in both traditional (Cohn et al., 1996) and deep Machine Learning (Gal et al., 2017b), including uncertainty-based approaches applied to image-segmentation pairs. In such methods, it is assumed that predictions with high uncertainty provide the most informative samples for training.

Evaluation Selecting the most informative samples for training contains two elements. Firstly, the uncertainty needs to be quantified. This is usually the predictive entropy Kasarla et al. (2019); Shen et al. (2021); Xie et al. (2022) or variance Ozdemir et al. (2021), but in some instances the epistemic uncertainty is explicitly estimated through Bayesian Active Learning by Disagreement (BALD) (Houlsby et al., 2011; Ma et al., 2024b; Shen et al., 2021). Simply stated, the reduction in posterior entropy indicates the informativeness of a data sample. In turn, this can also be formulated by the reduction in predictive entropy in the dual formulation. We can formally denote this as

$$\begin{aligned}
\text{BALD} &\equiv H[\boldsymbol{\theta}|\mathcal{D}] - \mathbb{E}_{p(\mathbf{y}|\mathbf{x}^*, \mathcal{D})}[H[\boldsymbol{\theta}|\mathbf{y}, \mathbf{x}^*, \mathcal{D}]], \\
&= H[\mathbf{y}|\mathbf{x}^*, \mathcal{D}] - H[\mathbf{y}|\boldsymbol{\theta}, \mathbf{x}^*, \mathcal{D}], \\
&= H[\mathbf{y}|\mathbf{x}^*, \mathcal{D}] - \mathbb{E}_{q(\boldsymbol{\theta}|\mathcal{D})}[H[\mathbf{y}|\mathbf{x}^*, \boldsymbol{\theta}]] = I(\mathbf{y}, \boldsymbol{\theta}|\mathbf{x}^*, \mathcal{D}).
\end{aligned} \tag{39}$$

Note the similarity between the mutual information I obtained from the predictive entropy decomposition in Equation (3), where both are the objective of epistemic uncertainty modeling. Secondly, to evaluate whether the active learning strategy is beneficial, the performance is mostly measured subject to increasingly stringent budget requirements (i.e. a percentage of the original dataset) Yang et al. (2017); Sourati et al. (2018); Kasarla et al. (2019); Mahapatra et al. (2018); Sinha et al. (2019); Siddiqui et al. (2020); Li & Alstrøm (2020); Kim et al. (2021); Shen et al. (2021); Burmeister et al. (2022); Ma et al. (2024b). Kahl et al. (2024) argue that Active Learning should be evaluated on image-level as humans dont annotate on pixel-level. Assuming a saturated performance on in-distribution data (training cycle t_1), the author propose to measure the improved relative performance, C , subject to a second training sample (t_2) from selected samples

$$C_{\text{total}} = C_{\text{method}} - C_{\text{random}}, \tag{40}$$

with

$$C = \frac{P_{t_2} - P_{t_1}}{P_{t_1}}, \tag{41}$$

where C_{method} denotes the relative improvement achieved by the employed method, and C_{random} is a correction term accounting for gains due to random sampling, and P suggested to be the Dice-score, but can theoretically be any segmentation metric.

Approaches Since the nature of this problem involves identifying and reducing model ignorance, the quantification of epistemic uncertainty is most appropriate. Hence, as can be seen in Table 2, most of the literature use MC dropout of ensembles. Furthermore, using the plain SoftMax activation has also been commonly used. Often, solely relying on the most uncertain samples can result in samples with limited

Table 3: Methods used for the application of Model Introspection

Method	Literature
VI	Ng et al. (2022); LaBonte et al. (2019)
LA	Zepf et al. (2023b)
TTA	Kahl et al. (2024); Wang et al. (2019b); Whitbread & Jenkinson (2022); Roshanzamir et al. (2023); Dahal et al. (2020)
Ensembling	Jungo et al. (2020); Mehrtash et al. (2020); Czolbe et al. (2021); Holder & Shafique (2021); Jungo & Reyes (2019); Ng et al. (2022); Hann et al. (2021); Jungo & Reyes (2019); Linmans et al. (2020); Pavlitskaya et al. (2020); Valada et al. (2017)
MC Dropout	Jungo et al. (2020); Kahl et al. (2024); Whitbread & Jenkinson (2022); Kendall et al. (2016); Kampffmeyer et al. (2016); Dechesne et al. (2021); Morrison et al. (2019); Qi et al. (2023); Eaton-Rosen et al. (2018); Jungo et al. (2018a;b); Roy et al. (2018a;b); Mehrtash et al. (2020); Nair et al. (2020); Sander et al. (2019); Hasan & Linte (2022b); Camarasa et al. (2021); Roshanzamir et al. (2023); Sedai et al. (2018); Seeböck et al. (2019); DeVries & Taylor (2018); Czolbe et al. (2021); Hoebel et al. (2019); Bhat et al. (2021); Dahal et al. (2020); Antico et al. (2020); Lambert et al. (2022); Hasan & Linte (2022a); Jungo & Reyes (2019); Ng et al. (2022); Iwamoto et al. (2021); Hoebel et al. (2020)
SSN	Kahl et al. (2024); Ng et al. (2022)
VAE	Chotzoglou & Kainz (2019); Viviers et al. (2023a); Czolbe et al. (2021); Bian et al. (2020)

diversity and therefore samples selected on the *representativeness* Ozdemir et al. (2021); Shen et al. (2021); Wu et al. (2021); Mahapatra et al. (2018); Sinha et al. (2019). Another crucial modeling element pertains the aggregation of the pixel-level uncertainties. Therefore, closeness to boundary Gorri et al. (2017); Kasarla et al. (2019); Ma et al. (2024b) or specific regions Gaillochet et al. (2023); Wu et al. (2021); Kasarla et al. (2019) are additionally incorporated when combining the uncertainty values across pixels. Siddiqui et al. (2020) determine the entropy through estimating the entropy across viewpoints in multi-view datasets. Gaillochet et al. (2023) argue the superiority of selecting samples based on batch-level uncertainty.

6.3 Model introspection

Erroneous predictions should correlate with the uncertainty in cases the source is assumed to be epistemic. In turn, this implies that the provided uncertainty can be used to gauge prediction quality of a model. High uncertainty predictions can be discarded to ensure a level of model reliability. Hence, the described problem can also be considered as Out-of-Distribution (OOD) detection (Lambert et al., 2022; Holder & Shafique, 2021). Including information on localized uncertainty to the training objective has shown to improve generalization capabilities (Ozdemir et al., 2017; Bian et al., 2020; Iwamoto et al., 2021; Li et al., 2021). Note that using uncertainty to guide model training is closely related to Active Learning, which has been discussed in Section 6.2.

Evaluation The relationship between uncertainty and model accuracy has been formalized by Mukhoti & Gal (2018) through the Patch Accuracy vs Patch Uncertainty (PAvPU) metric. Firstly, the accuracy given a certain prediction, $p(A|C)$, and secondly, the uncertainty given an inaccurate prediction $p(U|I)$. Given a threshold u_T that distinguishes certain from uncertain pixels or patches, we can define pixels that are accurate and certain, accurate and uncertain, inaccurate and certain, inaccurate and uncertain, denoted by u_{ac} , u_{au} , u_{ic} , u_{iu} , respectively. Consequently, the authors combine $p(A|C) = n_{ac}/(n_{ac} + n_{au})$ and $p(U|I) = n_{ic}/(n_{ic} + n_{iu})$ to obtain the Patch Accuracy vs Patch Uncertainty (PAvPU) metric, defined as

$$\text{PAvPU} = \frac{n_{ac} + n_{au}}{n_{ac} + n_{au} + n_{ic} + n_{iu}}. \quad (42)$$

It can be noted that uncertainty is usually only obtained on pixel basis, while crucial information can be present in structural statistics. Hence, Roy et al. (2018b) propose to use the Coefficient of Variation (CoV) addresses this by measuring structural uncertainty through dividing the volume variance over the mean for

Table 4: Methods used for the application of improved Model Generalization.

Method	Literature
SoftMax	Kasarla et al. (2019); García Rodríguez et al. (2020); Xie et al. (2022); Wu et al. (2021); Burmeister et al. (2022); Gaillochet et al. (2023)
SSN	Zepf et al. (2023a); Ng et al. (2022)
VAE	Viviers et al. (2023a); Zepf et al. (2023a); Hu et al. (2022)
DDPM	Wolleb et al. (2021); Wu et al. (2023b;a); Amit et al. (2021); Zbinden et al. (2023); Boggensperger et al. (2023); Hoogeboom et al. (2021)
MC dropout	Mukhoti & Gal (2018); Rumberger et al. (2020b); Saha et al. (2021a); Zhang et al. (2022a); Whitbread & Jenkinson (2022); Huang et al. (2018); Mukhoti et al. (2020); Ng et al. (2022); Wickström et al. (2020)
Ensembling	Ng et al. (2022); Larrazabal et al. (2021b); Kamnitsas et al. (2018); Saha et al. (2021b); Hu et al. (2023); Ji et al. (2021)
TTA	Wang et al. (2019a); Rakic et al. (2024); Whitbread & Jenkinson (2022)

all samples. The authors also evaluate structural uncertainties by assuming predictions with the pair-wise average overlap between all respective samples.

$$\bar{D} = \mathbb{E}_{p_{Y|X^*}} [\text{Dice}(t(y_i), t(y_j))] \quad \forall i \neq j. \quad (43)$$

Approaches Considering Table 3, it can be observed that epistemic methods such as MC dropout and Ensembles are by far the most popular choice of uncertainty encapsulation method. However, Concrete dropout (Rumberger et al., 2020b; Mukhoti & Gal, 2018), M-heads (auxiliary networks) (Jungo & Reyes, 2019; Limmans et al., 2020), MoE (Pavlitskaya et al., 2020) Laplace Approximation (Zepf et al., 2023b), Variational Inference in 3D (LaBonte et al., 2019), and test-time augmentation (Dahal et al., 2020) have also been used for this application.

6.4 Model generalization

As mentioned earlier in Section 5.1, sampling new parameter permutations often improves segmentation performance, due to the model combining effect. In contrast to other downstream tasks, evaluation does not require specialized metrics besides quantifying the relative change in model performance. For instance, dropout layers at the deeper decomposition levels of the SegNet (Badrinarayanan et al., 2015) improves model performance (Kendall et al., 2016). In Table 4, we can see improved performance with MC Dropout and also in specific with Concrete Dropout (Mukhoti & Gal, 2018; Rumberger et al., 2020b). The improved generalization from ensembling has also shown to produce more calibrated outputs (Mehrtash et al., 2020). Ng et al. (2022) found that ensembling results in the best performance improvement, while BBB is more robust to noise distortions. In other work, orthogonality within and across convolutional filters of the ensemble is enforced through minimizing their cosine similarity, which reaped similar merits (Larrazabal et al., 2021b). Ensembling has also been performed using M-Heads (Hu et al., 2023; Jungo & Reyes, 2019). Nonetheless, individual models in conventional ensembles receive data in an unstructured manner. Hence, specific subsets of the data can also be assigned to particular models with MoEs (Pavlitskaya et al., 2020; Ji et al., 2021; Gao et al., 2022). Generative models, though typically used for other applications, have also led to performance improvements across a wide range of studies Saha et al. (2021a); Wolleb et al. (2021); Wu et al. (2023b); Amit et al. (2021); Boggensperger et al. (2023); Zbinden et al. (2023); Viviers et al. (2023a); Zepf et al. (2023a); Hu et al. (2022).

6.5 Application domains

In this Table 5, we link the discussed methodologies and applications to their respective domains. It is evident that the medical domain, followed by the automotive field, is the most prominent for probabilistic segmentation tasks. The high-stakes nature of both domains contributes to their prominence, as uncertainty-aware models are especially vital in safety-critical applications. Specifically, the delineation of lung nodules in CT images are ambiguous. The LIDC-IDRI dataset is a multi-annotated Lung CT dataset, which serves as a good benchmark for quantifying observer variability and is reflected in the table.

Table 5: Overview that links literature to various domains and applications.

	Observer Variability	Active Learning	Model Introspection	Model Generalization
Outdoor scenes	Kahl et al. (2024); Kohl et al. (2019b); Kassapis et al. (2021); Gao et al. (2022)	Sinha et al. (2019); Kahl et al. (2024); Kasarla et al. (2019); Kim et al. (2021); Xie et al. (2022); Wu et al. (2021)	Pavlitskaya et al. (2020); Hasan & Linde (2022b); Sander et al. (2019); Ng et al. (2022); Hasan & Linde (2022a); Mehrash et al. (2020); Kendall et al. (2016); Kahl et al. (2024); Holder & Shafique (2021); Qi et al. (2023)	Ng et al. (2022); Huang et al. (2018); Zbinden et al. (2023); Mukhoti & Gal (2018); Amit et al. (2021); Hoogeboom et al. (2021); Valada et al. (2017); Rakic et al. (2024)
Indoor scenes		Siddiqui et al. (2020); Wu et al. (2021)	Qi et al. (2023)	
Various objects	Philps et al. (2024)		Kendall et al. (2016); Qi et al. (2023); Morrison et al. (2019)	
Remote sensing		García Rodríguez et al. (2020)	Dechesne et al. (2021;?); Kampffmeyer et al. (2016); Dechesne et al. (2021)	
Microscopy	Kohl et al. (2019a); Zepf et al. (2023a); Schmidt et al. (2023); Philps et al. (2024)	Khalili et al. (2024); Li & Alström (2020); Yang et al. (2017); Sadafi et al. (2019)	Limmans et al. (2020); Iwamoto et al. (2021)	Bogensperger et al. (2023); Amit et al. (2021)
Brain MRI	Philps et al. (2024); Bhat et al. (2023); Hu et al. (2023); Philps et al. (2024); Savadikar et al. (2021); Zhang et al. (2022c)	Zepf et al. (2023b); Ma et al. (2024b); Shen et al. (2021)	Roy et al. (2018b); Mehrash et al. (2020); Jungo & Reyes (2019); Eaton-Rosen et al. (2018); Wang et al. (2019b); Jungo et al. (2020); Whitbread & Jenkinson (2022); Monteiro et al. (2020); Lambert et al. (2022); Jungo et al. (2018b;a)	Wolleb et al. (2021); Wu et al. (2023b;a); Chen et al. (2023a); Wang et al. (2019a); Kamnitisas et al. (2018); Larrazabal et al. (2021b); Wang et al. (2019b); Whitbread & Jenkinson (2022)
Prostate MRI	Baumgartner et al. (2019); Hu et al. (2022; 2023); Zepf et al. (2024)	Burmeister et al. (2022); Gaillochet et al. (2023)	Mehrash et al. (2020); Zepf et al. (2023b)	Hu et al. (2022); Saha et al. (2021a); Rakic et al. (2024); Saha et al. (2021b)
Various MRI	Rahman et al. (2023)	Ozdemir et al. (2021); Hiasa et al. (2019); Ng et al. (2022); Burmeister et al. (2022); Ma et al. (2024b); Nath et al. (2020); Gaillochet et al. (2023)	Bhat et al. (2021); Camarasa et al. (2021); Nair et al. (2020); Roshanzamir et al. (2023); Hann et al. (2021)	Ji et al. (2021); Ng et al. (2022)
OCT imaging	Selvan et al. (2020)		Seeböck et al. (2019); Bian et al. (2020); Sedi et al. (2018)	Rakic et al. (2024); Ji et al. (2021); Wu et al. (2023a;b)
Dermoscopy		Li & Alström (2020); Gorri et al. (2017)	Zepf et al. (2023b); Jungo & Reyes (2019); DeVries & Taylor (2018); Czolbe et al. (2021)	Wu et al. (2023a); Zepf et al. (2023a)
Lung CT	Rafael-Palou et al. (2021); Gao et al. (2022); Valiuddin et al. (2024b); Chen et al. (2023a); Zhang et al. (2022b); Monteiro et al. (2020); Qiu & Lui (2020); Kohl et al. (2019a); Hu et al. (2022); Zhang et al. (2022c); Ganttenbein et al. (2020); Viviers et al. (2023b;c); Valiuddin et al. (2024a); Zbinden et al. (2023); Zepf et al. (2024); Kahl et al. (2024); Bhat et al. (2022a); Long et al. (2021b); Valiuddin et al. (2021); Rahman et al. (2023); Kohl et al. (2019b); Hu et al. (2023); Bhat et al. (2023); Kassapis et al. (2021); Long et al. (2021a); Selvan et al. (2020); Baumgartner et al. (2019)	Kahl et al. (2024); Hoebel et al. (2020)	Kahl et al. (2024); Czolbe et al. (2021); Chotzoglou & Kainz (2019)	Hu et al. (2022); Rakic et al. (2024); Zhang et al. (2022a)
Various CT	Valiuddin et al. (2024b); Hu et al. (2023;?)	Hiasa et al. (2019)	Hoebel et al. (2019); LaBonte et al. (2019;?)	Viviers et al. (2023a)
Various US	Rahman et al. (2023)	Yang et al. (2017)	Antico et al. (2020); Dahal et al. (2020); Bian et al. (2020)	Wu et al. (2023b;a); Rumberger et al. (2020b)
Others	Valiuddin et al. (2021)	Mahapatra et al. (2018)		Wickstrøm et al. (2020)

7 Discussion

This section builds on the reviewed theory and literature to guide researchers in selecting methods suited to their goals. Furthermore, it highlights key gaps and limitations, offering insights for addressing current challenges in the field and identifying promising directions for future research. Our main discussion points can be summarized as follows:

- The interpretation and quantification of epistemic and aleatoric uncertainty remain complex and warrant careful reconsideration, despite the literature often indicating a clear distinction between them. (Section 7.1).
- Spatial uncertainty introduces additional challenges, including the accurate estimation of structural entropy, the aggregation of pixel-wise uncertainties, and increased complexity in volumetric segmentation tasks (Section 7.2).
- Lack of standardization across the downstream tasks remains a major issue in the field, hindering fair benchmarking and limiting further progress (Section 7.3).
- Active Learning is a promising application of uncertainty quantification, reducing annotation costs while maintaining or even improving model generalization (Section 7.4).
- Segmentation backbones commonly used in the field tend to be outdated, with Transformer-based architectures having surpassed them in performance yet remaining underutilized in probabilistic dense predictions (Section 7.5).
- Aleatoric uncertainty is often modeled using conditional generative approaches; as this area advances rapidly, its developments should be promptly integrated into probabilistic segmentation research (Section 7.6).
- Alternatives to epistemic uncertainty modeling warrant further exploration due to longstanding criticisms of the predominantly used Monte Carlo dropout, questioning its ability to capture true model uncertainty (Section 7.7).

7.1 Disentangling uncertainties

Proper disentanglement of the uncertainties allows to accredit high-entropy outputs to either model ignorance about the data (epistemic), or inherent noise in the data generation process (aleatoric). Importantly, this distinction relates to the suggestion whether the uncertainty is reducible or not. Furthermore, Equation(2) indicates this can be achieved by introducing stochasticity into the model parameters or the features. Seemingly straightforward, sufficient literature and discussion in the scientific community exist related to the applicability of this taxonomy in practical cases. As paraphrased from Kirchhof et al. (2025), “*definitions of uncertainty resemble the shapes of clouds — clearly defined from a distance, but losing clarity during approach by dissolving in one another*”. We further explore this concept and show how confusion and contradiction have led to common pitfalls in related studies. To address these issues, we highlight key nuances in uncertainty modeling and contextualize this to segmentation problems by providing recommendations for future research.

7.1.1 Nuances in uncertainty modeling

Interpretation of uncertainty is task dependent It is essential to consider that interpretation of the uncertainty source often differs depending on the modeling context. For example, epistemic uncertainty to be considered as the number of required models to fit the data (Wimmer et al., 2023), evident in ensembling and M-head approaches for tasks related to model introspection and generalization (Sections 6.3 and 6.4). Another perspective pertains model disagreement (Houlsby et al., 2011; Gal et al., 2017b; Kirsch, 2024), relating to the source of observer variability (Section 6.1) and methods that employ mixture-of-expert approaches (Section 5.1.2). Also, it has been simply considered to be the remainder after subtracting the aleatoric from the total uncertainty Depeweg et al. (2018), such as commonly done in Active Learning (Section 6.2). Aleatoric uncertainty also knows several definitions such as being the Bayes-optimal residual risk Apostolakis

(1990); Helton (1997), but remains consistent in related literature as the inherent, irreducible noise in the data inducing variance in the ground-truth distribution (Section 6.1). However, it was highlighted that the decision to model a specific type of uncertainty was largely influenced by how the problem was framed. To avoid confusion, this task-dependency should be noted when interpreting uncertainty.

Interpretation of uncertainty is model dependent Moreover, past literature as well as our overview indicate the influence of specific design choices on the nature of the modeled uncertainty (Der Kiureghian & Ditlevsen, 2009). For instance, the expected entropy w.r.t. a stochastic parameter variable should represent the aleatoric uncertainty (Equation (3)). However, when employing generative models, this behavior changes. The latent (feature) stochasticity variable is employed to model the aleatoric uncertainty. Hence, the remaining uncertainty, i.e. epistemic, is encapsulated in the expected entropy w.r.t. this latent variable (Equation (13)). Hence, the calibration network of the GAN-based CAR model of Kassapis et al. (2021) (discussed in Section 4.2.1) actually quantified the epistemic rather than aleatoric uncertainty. This dependency is also demonstrated by the conflicting ideas on uncertainty encapsulated with TTA (Wang et al., 2019a; Ayhan & Berens, 2022; Zhang et al., 2022a; Wang et al., 2019b; Rakic et al., 2024; Kahl et al., 2024; Hu et al., 2022; Whitbread & Jenkinson, 2022; Roshanzamir et al., 2023). The key message thus far is that, after selecting the type of uncertainty to model, it is equally important to carefully choose the appropriate method for its representation, as confusion and misunderstandings can cause deviation from the targeted uncertainty type.

Uncertainties are intertwined Despite the seemingly rigorous and well-defined distinction, it can be seen that implementation rapidly blurs this notion. A systematic study has found that the ability to separate the uncertainties can strongly depend on the data Kahl et al. (2024). These findings are also supported by research presenting a strong correlation between epistemic and aleatoric uncertainty quantification methods de Jong et al. (2024); Mucsányi et al. (2024), indicating that they represent uncertainty of similar kind. Kendall & Gal (2017) have also observed that explicitly modeling a single uncertainty tends to compensate for the lack of the other. In probabilistic models, we can also find that the epistemic encapsulation methods have been used to model observer variability. Furthermore, using a combination of aleatoric and epistemic modeling techniques can also be beneficial (Gao et al., 2022). These findings further highlight the notion of the uncertainties being intertwined. On a slight side note, it is notable that popular BNN methods such as the Local Reparameterization trick use stochasticity in the output features of intermediate layers (usually considered to encapsulate aleatoric uncertainty) as a proxy to model the weight distributions Kingma et al. (2015), further supporting this argument.

Encapsulating vs. quantifying A common misconception pertains that modeling a specific uncertainty also implies that the predicted output represents that same uncertainty. This undermines the entropy decomposition in Equation (3) distinguishing between encapsulating, i.e. targeting an intended uncertainty type, versus quantifying, i.e. measuring the modeled uncertainty in isolation. For example, the estimation of mutual information is required to express the epistemic uncertainty in isolation. Nonetheless it is common for papers to quantify the uncertainty by inspecting the output distribution subject through repetitive sampling from the parameters densities, thereby approximating the predictive entropy encapsulating both uncertainties (Camarasa et al., 2021; Seeböck et al., 2019; Roshanzamir et al., 2023; Roy et al., 2018a; Rumberger et al., 2020b; Hoebel et al., 2022; Seeböck et al., 2019; Wundram et al., 2024b; Rumberger et al., 2020a; Sedai et al., 2018). At the very most, the output correlates with an increase in epistemic uncertainty. However, given the entanglement of both uncertainties, part of the predictive variance can be accredited to noise in the data. This similarly holds for literature emphasizing aleatoric uncertainty when estimating the predictive variance Zhang et al. (2022c); Monteiro et al. (2020); Valiuddin et al. (2024b); Gao et al. (2022). However, epistemic uncertainty is often assumed to be explained away or assumed to be comparatively negligible with large datasets. Finally, we have found it to be common to interchangeably use the total and model uncertainty, especially in the context of Monte Carlo Dropout methods Kendall et al. (2016); Roy et al. (2018b); DeVries & Taylor (2018); Mehrtash et al. (2020); Burmeister et al. (2022); Iwamoto et al. (2021). To prevent confusion in already established terminology, the term *model uncertainty* should be exclusively used for the induced ambiguity due to limited model complexity, rather than to denote general or the entire epistemic uncertainty.

7.1.2 Pragmatic use of uncertainty

Unless being the core contribution, there seems to be no compelling need to investigate uncertainty disentanglement for the applications of uncertainty in dense prediction. If performance on the downstream application is improved, it can be assumed that modeled uncertainty correlates with changes in variance of the predictive distribution. In such cases, no claims need to be made on the uncertainty type and neither is it required to isolate the two. Hence, as described in previous work, aleatoric and epistemic uncertainty should be used as to communicate whether the uncertainty is reducible or not (Der Kiureghian & Ditlevsen, 2009; Faber, 2005), to then select appropriate modeling methods.

As argued by Kahl et al. (2024), claiming to quantify an uncertainty type would ideally require validation across *all* relevant applications. For example, validation of epistemic uncertainty requires a clear distribution shift in the data (domain, semantic, covariate etc.), but it is often found in literature that either no distribution shift or the required metrics are used (Zhang et al., 2022a; Wang et al., 2019a; Postels et al., 2019; Mukhoti & Gal, 2018; Mobiny et al., 2021; Whitbread & Jenkinson, 2022). As discussed in Section 6.1, aleatoric uncertainty should be validated with multiple labels and appropriate metrics, but can often found to be evaluated on a single annotator or without the use of distribution-level statistics Wang et al. (2019a); Whitbread & Jenkinson (2022); Kendall & Gal (2017); Liu et al. (2022b); Schmidt et al. (2023); Savadikar et al. (2021). Hence, simply avoiding any serious claims related to either type alleviates this burden, and allows one to focus solely on the task at hand. In contrast to the work of Kahl et al. (2024), however, we do not consider calibration of models itself as a downstream task, but rather as a tool to gauge model reliability to be later used for other tasks. As a consequence, the pixel-wise uncertainties can be later used for possible downstream applications.

7.2 Spatial coherence

The inter-pixel dependency of segmentation masks often introduces additional complexity in proper uncertainty quantification, questioning the commonly repurposed techniques from conventional image-level classification. In this section, we further dive into import details and challenges arising due to the added dimension(s) in both 2D and 3D data.

Aggregation methods Quantifying the epistemic uncertainty requires subtracting the expected entropy from the total entropy of the predictive distribution (see equations (3) and (39)). In such cases, the entropy is usually estimated via mean or summation over all pixel-level uncertainty values Mukhoti & Gal (2018); Camarasa et al. (2021); Bhat et al. (2022b); Mukhoti et al. (2020); Ma et al. (2024b); Shen et al. (2021); Li & Alstrøm (2020); Dechesne et al. (2021); Huang et al. (2018); Nair et al. (2020); Zepf et al. (2023b). However, this asserts the assumption of a factorized categorical distribution, i.e. uncorrelated pixels, which is a strong assumption that ignores the core rationale for the field’s existence. Since this could explain failure cases of entropy-based uncertainty evaluation methods, it is important to shift towards contemporary generative models that enable exact likelihoods, improving the theoretical soundness of the evaluated entropies. Moreover, elements such as object class dependency, size, shape, proximity, contextual information etc. can all influence the decision-making of the aggregation method. Notably, Kahl et al. (2024) argue that pixel aggregation should be considered as a separate, distinct modeling choice in probabilistic segmentation. The authors demonstrate that naive summation-based aggregation techniques (Wang et al., 2019a; Jungo et al., 2020; Zhang et al., 2022a; Czolbe et al., 2021; Camarasa et al., 2021) can cause the foreground object size to correlate with the uncertainty score. Some empirical studies have explored aggregation (Camarasa et al., 2021; Roy et al., 2018b; Jungo et al., 2020; Kasarla et al., 2019; Xie et al., 2022; Wu et al., 2021). However, we advocate for deeper investigation into well-informed image-level aggregation strategies and their implications for uncertainty quantification.

Volumetric uncertainty modeling In clinical settings, data is often acquired volumetrically but sliced into patches due to memory limits. With improved compute, 3D segmentation models have gained traction for preserving spatial continuity and reducing inter-slice inconsistencies. As we have seen the implications of the additional dimension in 2D uncertainty, we similarly argue that 3D segmentation introduces or exacerbates previously mentioned issues related to entropy estimation and aggregation of pixels. Probabilistic

segmentation has been employed on 3D data but often are straightforward extensions of patch-wise segmentation architectures (Viviers et al., 2023b; Chotzoglou & Kainz, 2019; Long et al., 2021b; Saha et al., 2021a; 2020; Hoebel et al., 2019). Limited diversity of uncertainty-based sample selection in Active Learning requires more focus, since 2D slices of 3D volumes are often highly redundant Shen et al. (2021); Burmeister et al. (2022). Furthermore, given the high computational cost of many architectures, we emphasize the need for efficiency with higher-dimensional input tensors. Furthermore, methodologies need to be developed in order to appropriately compare 2D- to 3D models. For example, the GED cannot be estimated volumetrically with 2D models. Hence, general guidelines related to translating 2D segmentation models to 3D can be of great benefit for practitioners considering to phase out patch-based approaches for volumetric data. Fortunately, research dedicated to probabilistic volumetric segmentation is prevalent and its successes underline the potential for this research direction Liu et al. (2025); Burmeister et al. (2022); Viviers et al. (2023b).

7.3 Standardization

The widespread success of contemporary machine learning models can be largely attributed to open-source initiatives and rigorous benchmarking practices. The field of probabilistic segmentation falls short on this. A key factor contributing to these diverging standards is that the literature is predominantly application-driven, uncertainty often considered merely an auxiliary tool, leading to a fragmented landscape where studies rely on varied datasets and methodologies without a shared evaluation protocol. This problem has been partly addressed by contemporary research attempting to standardize the field through a unified framework after identifying key pitfalls (Kahl et al., 2024). These practices are included in our recommended practices, as discussed in Section 6 per application.

Despite the aforementioned points, efforts to quantify observer variability show some implicit consensus. Notably, the recommendations of Kahl et al. (2024) diverge from these practices, suggesting a more rigorous examination of this application. For instance, for the widely used LIDC-IDRI dataset (Armato, 2011), we recommend following the preprocessing protocol of Baumgartner et al. (2019), which is supported by publicly available code and has been adopted in several subsequent studies. Similarly, the Cityscapes dataset (Cordts et al., 2016a), comprising street-view images from German cities, has been used to introduce artificial class-level label ambiguity (Kassapis et al., 2021; Kohl et al., 2019b; Gao et al., 2022). We advise using the label-switching parameters proposed by Kohl et al. (2019b), whose preprocessing scripts are also available. Other multi-annotated datasets, such as those from the QUBIQ Challenge (noa), include MRI and CT scans of various organs (Valiuddin et al., 2024b; Ji et al., 2021), although they follow less standardized preprocessing. The RIGA dataset for retinal fundus images (Almazroa et al., 2018) can be used as in Wu et al. (2022).

The evaluation metrics used across studies also diverge substantially. While GED and Hungarian Matching are commonly applied to assess model performance, key details—such as the choice of distance kernel, the number of predictive samples, and the handling of correct empty segmentations (which cause NaNs) vary widely. This inconsistency is particularly evident in the work of Zbinden et al. (2023), who attempt to identify common ground across benchmarks but find over 10 (!) different evaluation methods. Additionally, many reported results are not taken from original papers but from follow-up studies using them as baselines. See Table 6 for a comparison of benchmarks on the LIDC-IDRI dataset. We recommend using 16 predictive samples as the standard for evaluating the LIDC-IDRI (v2, see experiments section of Zbinden et al. (2023)) dataset. Additionally, correctly predicted empty segmentations should be assigned full score. Notably, the literature often overemphasizes metric improvement, which can incentivize models to simply replicate ground-truth masks rather than capture the underlying distribution. This risks undermining the original goal of predicting plausible, unseen segmentations, a textbook case of Goodhart’s law: “*When a measure becomes a target, it ceases to be a good measure*” and is further compounded by known biases in commonly used metrics (Kohl et al., 2019a; Zepf et al., 2023a; Valiuddin et al., 2024b;a). Hence, practitioners should remain cautious and complement quantitative evaluations with qualitative assessments from domain experts.

7.4 Future of Active Learning

Among the applications considered, uncertainty quantification emerges as a promising approach to Active Learning, showing true potential of potentially reducing annotation costs while preserving or even improving model generalization. Active Learning directly addresses the labeling bottleneck through uncertainty-driven selection, aligning with model introspection and fostering human-AI collaboration in specialized domains. Furthermore, when combined with federated learning, this field can accelerate privacy-centric collaboration by enabling efficient, human-in-the-loop improvement of safety-critical models across decentralized data silos. However, key limitations remain and require further research.

Model sensitivity and baselines While deep learning-based segmentation typically involves high-dimensional data and large datasets, active learning requires a well-generalized model trained on limited data. This mismatch renders performance highly sensitive to budget constraints, model architecture, hyperparameters, and regularization Mittal et al. (2019); Kirsch (2024); Munjal et al. (2022); Kirsch et al. (2019); Gaillochet et al. (2023). Furthermore, random sampling, particularly when combined with MC Dropout, often proves to be a surprisingly strong baseline that is difficult to outperform Kahl et al. (2024); Mittal et al. (2019); Lüth et al. (2023); Burmeister et al. (2022); Siddiqui et al. (2020); Kim et al. (2021); Sinha et al. (2019); Nath et al. (2020), especially with highly imbalanced data Ma et al. (2024a). This observation can partly be attributed to the fact that MC Dropout likely fails to capture true Bayesian uncertainty (see Section 7.7), inviting exploration of other techniques.

Sample informativeness Besides uncertainty, the diversity of selected samples is equally critical. For instance, a set of highly uncertain samples may share similar semantic content, leading the model to overfit a narrow and homogeneous region of the data distribution during early training. Hence, sample selection should be based on both uncertainty and diversity (Ozdemir et al., 2021; Wu et al., 2021; Jensen et al., 2019; Burmeister et al., 2022). Ozdemir et al. (2021) leverage the latent space of a VAE to select representative samples, whereas other studies use feature vectors from prediction models (Wu et al., 2021; Burmeister et al., 2022). Owing to their significantly greater representational capacity, modern generative models, as discussed in Section 7.6, merit experimental investigation together with segmentation specific conditioning. Furthermore, the sample diversity offered by such models can be effectively combined with adversarial training (Mahapatra et al., 2018; Sinha et al., 2019).

Uncertainty calibration and aggregation As discussed in Section 4.1, using the predictive entropy of SoftMax-based uncertainty requires proper calibration. Unfortunately, this is rarely verified in prac-

Table 6: Comparison of test evaluations on two versions of the LIDC-IDRI dataset. Table extended from (Zbinden et al., 2023). *Indicates evaluation results not obtained from the original work.

Method	LIDCv1		LIDCv2	
	GED ₁₆	HM-IoU ₁₆	GED ₁₆	HM-IoU ₁₆
PU-Net (Kohl et al., 2019b)	0.310 ± 0.010*	0.552 ± 0.000*	0.320 ± 0.030*	0.500 ± 0.030*
HPU-Net (Kohl et al., 2019a)	0.270 ± 0.010*	0.530 ± 0.010*	0.270 ± 0.010*	0.530 ± 0.010*
PhiSeg (Baumgartner et al., 2019)	0.262 ± 0.000*	0.586 ± 0.000*	-	-
SSN (Monteiro et al., 2020)	0.259 ± 0.000*	0.558 ± 0.000*	-	-
CAR (Kassapis et al., 2021)	-	-	0.264 ± 0.002	0.592 ± 0.005
JProb. U-Net (Zhang et al., 2022d)	-	-	0.262 ± 0.000	0.585 ± 0.000
PixelSeg (Zhang et al., 2022c)	0.243 ± 0.010	0.614 ± 0.000	0.260 ± 0.000	0.587 ± 0.010
MoSE (Gao et al., 2022)	0.218 ± 0.001	0.624 ± 0.004	-	-
AB (Chen et al., 2022)	0.213 ± 0.001*	0.614 ± 0.001*	-	-
CIMD (Rahman et al., 2023)	0.234 ± 0.005*	0.587 ± 0.001*	-	-
CCDM (Zbinden et al., 2023)	0.212 ± 0.002	0.623 ± 0.002	0.239 ± 0.003	0.598 ± 0.001
BerDiff (Chen et al., 2023a)	-	-	0.238 ± 0.010	0.596 ± 0.000
MedSegDiff (Wu et al., 2023b)	-	-	0.420 ± 0.030*	0.413 ± 0.030*
SPU-Net (Valiuddin et al., 2024b)	-	-	0.327 ± 0.003	0.560 ± 0.005

tice Kasarla et al. (2019); García Rodríguez et al. (2020); Xie et al. (2022); Wu et al. (2021); Burmeister et al. (2022); Gaillochet et al. (2023). Furhtermore, most works rely on heuristics to aggregate the pixel-level information such as closeness to edges, boundaries or the use of super-pixels Gorri et al. (2017); Kasarla et al. (2019); Ma et al. (2024b); Gaillochet et al. (2023); Wu et al. (2021); Kasarla et al. (2019); Bengar et al. (2021). Moreover, the mutual information is often quantified by plain summation (i.e. assuming pixel independence) Shen et al. (2021); Ma et al. (2024b). We hypothesize that these ad-hoc aggregation techniques, as mentioned in Section 7.2, are a key limiting factor to uncertainty-based Active Learning.

The Cold-Start Problem Finally, the “cold start” problem Nath et al. (2022); Houlsby et al. (2014); Yuan et al. (2020a), the notion that uncertainty methods work poor on the initial samples, is rarely addressed. Most approaches assume a well-trained model is already available, yet methods like MC Dropout require warm-up epochs to yield meaningful uncertainty. Addressing this gap, post-hoc techniques such as that of Sourati et al. (2018), which enable uncertainty estimation from pretrained deterministic networks, represent a valuable and underexplored direction for early-stage sample selection.

7.5 Segmentation backbone

Due to emphasis on the uncertainty methods, the backbone feature extractor is often an overlooked element in uncertainty modeling. For example, CNN-based encoder-decoder models such as the U-Net, remain the preferred backbone architecture (Eisenmann et al., 2023). Nevertheless, Vision Transformers (ViTs) (Dosovitskiy et al., 2020) such as SegFormer, Swin U-Net, Mask2Former already outperform CNNs in general segmentation problems (Xie et al., 2021; Zhang & Yang, 2021; Cheng et al., 2022). With the exception of experiments in Kahl et al. (2024) (combining SSN (Monteiro et al., 2020) with HRNet (Yuan et al., 2020b)), all employed models use a CNN backbone. The limited adoption of ViTs likely stems from CNNs’ advantageous inductive biases, whereas Transformers typically require extensive pretraining on large datasets (Caron et al., 2021). Therefore, we recommend integrating the discussed methods into similar architectures to achieve both strong classification performance and effective ambiguity modeling. Also, CNNs have benefited from the recent developments in Transformers. For instance, *ConvNext* takes inspiration from contemporary Transformers to modernize existing ResNet-based CNNs, retaining the inductive biases of convolutional filters and achieving significant performance gains (Liu et al., 2022c). These same inductive biases have been added to ViTs through CNN adapters to also enhance performance Chen et al. (2023b).

7.6 Modeling feature distributions

In many instances, latent-variable models are employed to model the observer variability. To aid with appropriate model selection, we will discuss the strengths and weaknesses of each of those approaches. A summary of this discussion is presented in Table 7. Note that, while classified PixelCNNs and SSNs are classified as *pixel-level* methods, both can also be phrased as a latent-variable model.

ELBO suboptimality Known for its flexibility to various datasets, fast sampling time and the interpretable latent space, VAEs seem to be the most popular choice for aleatoric uncertainty quantification. Nonetheless, the shortcomings of VAEs are well known. For example, such models suffer from inference sub-optimality related to ELBO optimization Cremer (2018); Zhao et al. (2017) and literature on the VAE-based PU-Net often describe behavior similar to the well-known phenomena of *model collapse* Valiuddin et al. (2024a;b); Qiu & Lui (2020). This has been hypothesized to be caused by excessively strong decoders Chen et al. (2016) and is especially apparent when dealing with complex hierarchical decoding structures, where additional modifications such as the GECO objective Kohl et al. (2019a), residual connections Kohl et al. (2019a); Baumgartner et al. (2019), or deep supervision Baumgartner et al. (2019) are required for generalization. A unique benefit of this approach is the ability to semantically interpret the latent space with, for example, interpolation between annotation styles or the exploration of low-likelihood regions.

Limitation of sequential modeling The adoption of sequential sampling models DDPMs or PixelSeg is rather limited compared to the VAE-based models. This is unexpected, as both models outperforms the latter. This is likely due to their tedious sequential inference procedure Song et al. (2020); Zheng et al.

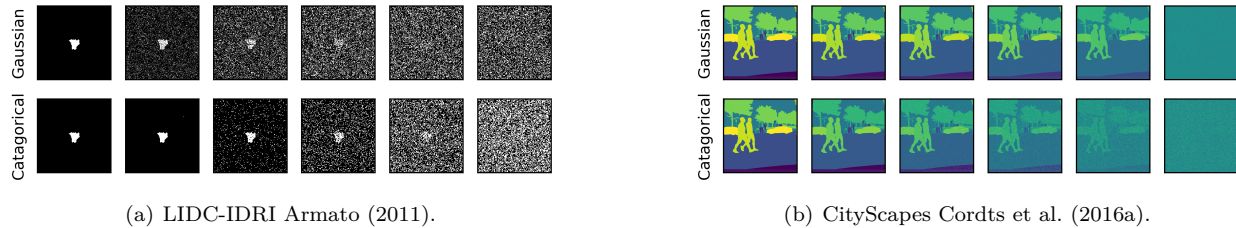


Figure 13: Continuous vs. categorical forward diffusion process with cosine noise scheduling Nichol & Dhariwal (2021). Note the use of categorical diffusion that results in a more gradual transition for the multi-class case.

(2023); Meng et al. (2023); Zhang et al. (2022c), a crucial limitation that is exacerbated in supervised settings, which often require validation through sampling on a separate data split. Despite these shortcomings, the strengths of DDPMs should not be overlooked. Their iterative sampling allows for highly flexible modeling and preserves high-frequency details often lost in latent-variable approaches like VAEs, which can produce blurry reconstructions. Furthermore, recent advances in faster sampling methods, such as DDIMs (Song et al., 2020) and Flow Matching Lipman et al. (2022), make these models promising candidates for further exploration.

Discrete vs. continuous It can be noted in Table 6 that the best-performing DDPM models are discrete in nature Chen et al. (2023a); Zbinden et al. (2023). While it is debatable whether shifting to categorical distributions is required for complex image generation Chen et al. (2022). Visually, this can be already quite apparent for the multi-class case, where the transition to noise is visually more gradual in the discrete transition (see Figure 13). However, Table 1 shows AB Chen et al. (2022) performs almost identically to CCDM Zbinden et al. (2023), suggesting that straightforward thresholding of continuous models have little-to-no performance sacrifice compared with explicitly modeling discrete distributions. These observations call for further investigation of the merits of categorical distributions in segmentation settings.

Others Stochastic Segmentation Networks (SSNs) are a simple, fast, and model-agnostic approach for modeling uncertainty. However, they can suffer from training instability due to the requirement that the covariance matrix be invertible. To address this limitation, the authors propose masking out the background to avoid exploding variances and using uncorrelated Gaussians when the covariance matrix is singular. Despite these efforts, SSNs scale poorly with data, and a potential solution is to shift the stochasticity deeper into the network by introducing a latent prior, resembling VAE-based models but with a more complex latent space. CAR, on the other hand, is a less commonly used method, likely due to the well-known instability of GAN-based models Arjovsky & Bottou (2017). GANs often require additional heuristic terms in the loss function to ensure stable training. CAR is no exception to this, as its objective function combines four separate losses.

Recommendation We advocate for a deeper contextualization of contemporary generative modeling research within probabilistic segmentation models. Generative modeling is a rapidly evolving field and any such model can be modified for segmentation through intricate conditioning. For example, DDPMs were initially proposed for general image generation (Ho et al., 2020), but was quickly adopted for stochastic segmentation. Furthermore, flow-based models also enjoy many benefits yet to be explored in this field, such as exact likelihood modeling and faster sampling Lipman et al. (2022). In terms of model selection, we have noticed SSN being the most practical solution across literature due to being model agnostic and receiving good benchmarking scores (Kahl et al., 2024; Monteiro et al., 2020; Ng et al., 2022).

7.7 Modeling parameter distributions

In the previous sections, we reviewed feature modeling methods, typically used to quantify observer variability. Other downstream applications usually rely on epistemic uncertainty modeling, i.e. modeling parameter distributions, which will be discussed in this section.

Criticism of MC Dropout Nearly all literature on epistemic uncertainty quantification relies on approximations of variational inference (VI). Among these, MC Dropout is the most commonly used due to its simplicity, low computational cost, and ease of implementation. However, MC Dropout has faced substantial criticism Folgoc et al. (2021); Osband (2016); Kingma et al. (2015); Gal et al. (2017a). For instance, it can assign zero probability to the true posterior or introduce erroneous multi-modality Folgoc et al. (2021). It is also sensitive to model size and dropout rate rather than the observed data Osband (2016); Kingma et al. (2015). To address these issues, some alternatives attempt to learn the dropout rate Kingma et al. (2015); Gal et al. (2017a). Still, uncertainty estimates from MC Dropout should be treated as a convenient byproduct—not a reliable core feature. When precise uncertainty quantification is critical, such methods are generally insufficient and best avoided. When uncertainty modeling is used to boost model performance, rigorous benchmarking of uncertainty often becomes secondary. In such cases, methods like MC Dropout are treated as regularization tools being part of the deep learning toolbox, rather than for genuine uncertainty estimation. However, it’s debatable whether the performance gains stem from better uncertainty modeling or from other factors. For instance, both ensembling and MC Dropout introduce a model combination effect—effectively averaging multiple networks. MC Dropout also resembles placing an L_2 penalty on weights. While these effects can improve generalization, similar gains might be achieved with simpler, more efficient regularizers. Perhaps it is the stochasticity itself that helps. Still, if performance is the main goal, uncertainty modeling is likely not the most efficient route due to its added computational cost. Instead, improved performance may simply be a side effect of these techniques.

Comparative studies Finally, the optimal method for uncertainty quantification has yet to be determined. In some works, MC dropout was found to perform better than ensembling Hoebel et al. (2020); Roy et al. (2018b), while in other works ensembling excels Mehrtash et al. (2020); Ng et al. (2022). Finally, there is convincing evidence to prefer Concrete Dropout rather than MC Dropout Mukhoti & Gal (2018). All things considered, the preference for a particular methodology seems to carry a strong data-dependency Da-

Table 7: Comparison between generative models that model aleatoric uncertainty.

Method	Advantages	Disadvantages	Examples
SSN	Model agnostic, explicit likelihoods, fast sampling	possibly unstable, memory intensive	(Monteiro et al., 2020; Kahl et al., 2024; Zepf et al., 2023a; Philips et al., 2024; Kahl et al., 2024)
PixelCNN	Explicit, exact likelihoods	Sequential sampling, memory intensive	Zhang et al. (2022c)
GAN	Fast sampling, flexible	Unstable training, poorly defined objective, implicit likelihoods	(Kassapis et al., 2021; Isola et al., 2017)
VAE	Fast sampling, flexible, interpretable latent space, ELBO	Mode/posterior collapse, amortization gap	(Kohl et al., 2019b; Selvan et al., 2020; Valiuddin et al., 2021; 2024a; Qiu & Lui, 2020; Bhat et al., 2022a; 2023; Valiuddin et al., 2024b; Zhang et al., 2022b; Kohl et al., 2019a; Baumgartner et al., 2019; Hu et al., 2023; Liu et al., 2022b; Fischer et al., 2023; Savadikar et al., 2021; Rafael-Palou et al., 2021; Viviers et al., 2023b;a; Chotzoglou & Kainz, 2019; Saha et al., 2021a;b; Long et al., 2021a; Schmidt et al., 2023; Savadikar et al., 2021; Rafael-Palou et al., 2021; Zepf et al., 2024; 2023a; Hu et al., 2022)
DDPM	Flexible, expressive	Sequential sampling	(Chen et al., 2023a; Zbinden et al., 2023; Rahman et al., 2023)

hal et al. (2020); Jungo & Reyes (2019). A valuable contribution to the field pertains a comprehensive benchmark paper, which compares all available epistemic uncertainty quantification methods across a wide range of datasets. In particular, such study can elucidate the data-dependent preference for specific methodologies (i.e. why ensembling or MC Dropout is often preferred). Additionally, recent studies have shown the benefits of moving from a few large, to many small experts when using an MoE ensemble for language modeling (He, 2024). Future work should also experiment with this.

Alternatives to Variational Inference Approaches besides VI, such as Markov Chain Monte Carlo (MCMC) or Laplace Approximations, are also viable options to approximate the Bayesian posterior. Especially the Laplace Approximation can be very beneficial, as it is easily applicable to pretrained networks. Notably, both Laplace Approximation and VI are biased and operate in the neighborhood of a single mode, while MCMC methods are a more attractive option when expecting to fit multi-modal parameter distributions. Zepf et al. (2023b) explored the impact of the Laplace Approximation on segmentation networks; however, beyond this work, the method has received limited attention in the field.

Sampling-free uncertainty The multiple forward passes required in many Bayesian uncertainty quantification can incur cumbersome additional costs. Hence, considerable efforts have been made towards sampling-free uncertainty models (Mukhoti et al., 2023; Liu et al., 2020; Van Amersfoort et al., 2020; Postels et al., 2019), only depending on a single forward pass. Mukhoti et al. (2023) show that Gaussian Discriminant Analysis after training with SoftMax predictive distribution can in some instances surpass methods such as MC Dropout and ensembling. Along similar lines, Evidential Deep Learning also possesses the advantage of quantifying both uncertainties with a single forward pass. This framework is based on a generalization of Bayes theorem, known as the Dempster-Shafer Theory of Evidence (DST) (Dempster, 1967). While common in Bayesian probability, DST does not require prior probabilities and bases subjective probabilities on belief masses assigned on a frame of discernment, i.e. the set of all possible outcomes. The use of Evidential Deep Learning has seen success in conventional classification problems (Sensoy et al., 2018), and Ancha et al. (2024) recently applied this concept to segmentation to decouple aleatoric and epistemic uncertainty within a single model. However, follow-up research in this direction remains limited to date.

Reliable uncertainty estimates A distribution-free framework known as Conformal Prediction (CP) produces prediction sets that guarantee inclusion of the ground truth with a user-specified probability. By using an additional calibration set, CP transforms heuristic model confidence scores into rigorous uncertainty estimates. This technique is particularly renowned for being model-agnostic, simple, and highly flexible (Angelopoulos & Bates, 2021). Recently, CP has been applied to segmentation tasks (Wieslander et al., 2020; Brunekreef et al., 2024; Mossina et al., 2024; Wundram et al., 2024a), benefiting from these advantages and reflecting the growing interest in the framework for structured prediction. We encourage further research to explore novel applications and benchmark CP against existing architectures.

8 Conclusion

Modeling the uncertainty of segmentation models is essential for accurately assessing the reliability of their predictions. Given the vast and diverse body of related literature spanning various applications and modalities, often scattered and marked by inconsistent evaluation and benchmarking practices, there is a clear need for a comprehensive and systematic overview. This work addresses that need by presenting clear definitions and a unified notation for methodologies in uncertainty modeling. Furthermore, confusion and misunderstanding around uncertainty modeling and quantification have led to diverging beliefs within the field. By structuring the methodologies by targeted uncertainty type and followed by downstream pipeline into four distinct tasks, it becomes easier for researchers to navigate the field and build upon existing work. We place particular emphasis on addressing key conceptual gaps to support both pragmatic and theoretically sound research. We also highlight the potential and broader impact of advancing uncertainty-based active learning. A noticeable trend is the adaptation of generative modeling advances to segmentation through novel, task-specific conditioning strategies for modeling ambiguity in segmentation masks. While such efforts are already underway, it remains important to closely follow progress in general generative machine learning and continue exploring its effective application to segmentation. Finally, we recommend future work to focus on improving spatial aggregation methods, standardization in benchmarking, backbone architectures, as well as the adoption of novel uncertainty estimation techniques, as many commonly used methods lack rigor. In particular, there is growing interest in distribution- and sampling-free approaches. In this manner, this review paper aims to guide researchers toward building more reliable, efficient, and uncertainty-aware segmentation models within the lightning-fast evolving field of Deep Learning-based Computer Vision.

References

QUBIQ 2021. URL <https://qubiq21.grand-challenge.org/QUBIQ2021/>.

Ahmed Almazroa, Sami Alodhayb, Essameldin Osman, Eslam Ramadan, Mohammed Hummadi, Mohammed Dlaim, Muhamad Alkatee, Kaamran Raahemifar, and Vasudevan Lakshminarayanan. Retinal fundus images for glaucoma analysis: the riga dataset. In *Medical Imaging 2018: Imaging Informatics for Healthcare, Research, and Applications*, volume 10579, pp. 55–62. SPIE, 2018.

Tomer Amit, Tal Shaharbany, Eliya Nachmani, and Lior Wolf. Segdiff: Image segmentation with diffusion probabilistic models. *arXiv preprint arXiv:2112.00390*, 2021.

Siddharth Ancha, Philip R Osteen, and Nicholas Roy. Deep evidential uncertainty estimation for semantic segmentation under out-of-distribution obstacles. In *Proc. IEEE Int. Conf. Robot. Autom.*, 2024.

Anastasios N Angelopoulos and Stephen Bates. A gentle introduction to conformal prediction and distribution-free uncertainty quantification. *arXiv preprint arXiv:2107.07511*, 2021.

Maria Antico, Fumio Sasazawa, Yu Takeda, Anjali Tumkur Jaiprakash, Marie-Luise Wille, Ajay K Pandey, Ross Crawford, Gustavo Carneiro, and Davide Fontanarosa. Bayesian cnn for segmentation uncertainty inference on 4d ultrasound images of the femoral cartilage for guidance in robotic knee arthroscopy. *IEEE access*, 8:223961–223975, 2020.

George Apostolakis. The concept of probability in safety assessments of technological systems. *Science*, 250 (4986):1359–1364, 1990.

Martin Arjovsky and Léon Bottou. Towards principled methods for training generative adversarial networks. *arXiv preprint arXiv:1701.04862*, 2017.

Samuel Armato. The Lung Image Database Consortium (LIDC) and Image Database Resource Initiative (IDRI): A Completed Reference Database of Lung Nodules on CT Scans: The LIDC/IDRI thoracic CT database of lung nodules. *Medical Physics*, 38(2):915–931, January 2011. ISSN 00942405. doi: 10.1118/1.3528204.

Murat Seckin Ayhan and Philipp Berens. Test-time data augmentation for estimation of heteroscedastic aleatoric uncertainty in deep neural networks. In *Medical Imaging with Deep Learning*, 2022.

Vijay Badrinarayanan, Alex Kendall, and Roberto Cipolla. Segnet: A deep convolutional encoder-decoder architecture for image segmentation. *IEEE Trans. Pattern Anal. Mach. Intell.*, 39:2481–2495, 2015.

Christian F Baumgartner, Kerem C Tezcan, Krishna Chaitanya, Andreas M Hötker, Urs J Muehlematter, Khoshy Schawkat, Anton S Becker, Olivio Donati, and Ender Konukoglu. Phiseg: Capturing uncertainty in medical image segmentation. In *MICCAI*, pp. 119–127. Springer, 2019.

Javad Zolfaghari Bengar, Joost van de Weijer, Bartlomiej Twardowski, and Bogdan Raducanu. Reducing label effort: Self-supervised meets active learning. In *Proceedings of the IEEE/CVF International Conference on Computer Vision*, pp. 1631–1639, 2021.

Ishaan Bhat, Hugo J Kuijf, Veronika Cheplygina, and Josien PW Pluim. Using uncertainty estimation to reduce false positives in liver lesion detection. In *2021 IEEE 18th International Symposium on Biomedical Imaging (ISBI)*, pp. 663–667. IEEE, 2021.

Ishaan Bhat, Josien PW Pluim, and Hugo J Kuijf. Generalized probabilistic u-net for medical image segmentation. In *UNSURE workshop, MICCAI*, pp. 113–124. Springer, 2022a.

Ishaan Bhat, Josien PW Pluim, Max A Viergever, and Hugo J Kuijf. Influence of uncertainty estimation techniques on false-positive reduction in liver lesion detection. *arXiv preprint arXiv:2206.10911*, 2022b.

Ishaan Bhat, Josien P. W. Pluim, Max A. Viergever, and Hugo J. Kuijf. Effect of latent space distribution on the segmentation of images with multiple annotations, April 2023. arXiv:2304.13476 [cs, eess].

Cheng Bian, Chenglang Yuan, Jiexiang Wang, Meng Li, Xin Yang, Shuang Yu, Kai Ma, Jin Yuan, and Yefeng Zheng. Uncertainty-aware domain alignment for anatomical structure segmentation. *Medical Image Analysis*, 64:101732, August 2020. ISSN 13618415. doi: 10.1016/j.media.2020.101732.

Christopher M Bishop. *Neural networks for pattern recognition*. Oxford university press, 1995.

Charles Blundell, Julien Cornebise, Koray Kavukcuoglu, and Daan Wierstra. Weight uncertainty in neural network. In *ICML*, pp. 1613–1622. PMLR, 2015.

Lea Bogensperger, Dominik Narnhofer, Filip Ilic, and Thomas Pock. Score-Based Generative Models for Medical Image Segmentation using Signed Distance Functions, March 2023. arXiv:2303.05966 [cs].

Aleksandar Botev, Hippolyt Ritter, and David Barber. Practical gauss-newton optimisation for deep learning. In *Proceedings of the 34th International Conference on Machine Learning (ICML)*, 2017.

Olivier Bousquet, Sylvain Gelly, Ilya Tolstikhin, Carl-Johann Simon-Gabriel, and Bernhard Schoelkopf. From optimal transport to generative modeling: the vegan cookbook. *arXiv preprint arXiv:1705.07642*, 2017.

Yuri Boykov, Olga Veksler, and Ramin Zabih. Fast approximate energy minimization via graph cuts. *IEEE ICCV*, 1:377–384 vol.1, 2001.

Joren Brunekreef, Eric Marcus, Ray Sheombarsing, Jan-Jakob Sonke, and Jonas Teuwen. Kandinsky conformal prediction: Efficient calibration of image segmentation algorithms. In *Proceedings of the IEEE/CVF Conference on Computer Vision and Pattern Recognition*, pp. 4135–4143, 2024.

Josafat-Mattias Burmeister, Marcel Fernandez Rosas, Johannes Hagemann, Jonas Kordt, Jasper Blum, Simon Shabo, Benjamin Bergner, and Christoph Lippert. Less is more: A comparison of active learning strategies for 3d medical image segmentation. *arXiv preprint arXiv:2207.00845*, 2022.

Robin Camarasa, Daniel Bos, Jeroen Hendrikse, Paul Nederkoorn, M Eline Kooi, Aad van der Lugt, and Marleen de Bruijne. A quantitative comparison of epistemic uncertainty maps applied to multi-class segmentation. *arXiv preprint arXiv:2109.10702*, 2021.

Mathilde Caron, Hugo Touvron, Ishan Misra, Hervé Jégou, Julien Mairal, Piotr Bojanowski, and Armand Joulin. Emerging properties in self-supervised vision transformers. In *Proceedings of the IEEE/CVF international conference on computer vision*, pp. 9650–9660, 2021.

Liang-Chieh Chen, George Papandreou, Florian Schroff, and Hartwig Adam. Rethinking atrous convolution for semantic image segmentation. *arXiv preprint arXiv:1706.05587*, 2017.

Tao Chen, Chenhui Wang, and Hongming Shan. BerDiff: Conditional Bernoulli Diffusion Model for Medical Image Segmentation, April 2023a. arXiv:2304.04429 [cs].

Ting Chen, Ruixiang Zhang, and Geoffrey Hinton. Analog bits: Generating discrete data using diffusion models with self-conditioning. *arXiv preprint arXiv:2208.04202*, 2022.

Xi Chen, Diederik P Kingma, Tim Salimans, Yan Duan, Prafulla Dhariwal, John Schulman, Ilya Sutskever, and Pieter Abbeel. Variational lossy autoencoder. *arXiv preprint arXiv:1611.02731*, 2016.

Zhe Chen, Yuchen Duan, Wenhui Wang, Junjun He, Tong Lu, Jifeng Dai, and Yu Qiao. Vision transformer adapter for dense predictions, 2023b. URL <https://arxiv.org/abs/2205.08534>.

Bowen Cheng, Ishan Misra, Alexander G Schwing, Alexander Kirillov, and Rohit Girdhar. Masked-attention mask transformer for universal image segmentation. In *Proceedings of the IEEE/CVF conference on computer vision and pattern recognition*, pp. 1290–1299, 2022.

Elisa Chotzoglou and Bernhard Kainz. Exploring the relationship between segmentation uncertainty, segmentation performance and inter-observer variability with probabilistic networks. In *LABELS, MICCAI*, pp. 51–60. Springer, 2019.

Bertrand Clarke. Comparing bayes model averaging and stacking when model approximation error cannot be ignored. *Journal of Machine Learning Research*, 4(Oct):683–712, 2003.

David A Cohn, Zoubin Ghahramani, and Michael I Jordan. Active learning with statistical models. *Journal of artificial intelligence research*, 4:129–145, 1996.

Marius Cordts, Mohamed Omran, Sebastian Ramos, Timo Rehfeld, Markus Enzweiler, Rodrigo Benenson, Uwe Franke, Stefan Roth, and Bernt Schiele. The cityscapes dataset for semantic urban scene understanding. *IEEE/CVF CVPR*, pp. 3213–3223, 2016a.

Marius Cordts, Mohamed Omran, Sebastian Ramos, Timo Rehfeld, Markus Enzweiler, Rodrigo Benenson, Uwe Franke, Stefan Roth, and Bernt Schiele. The Cityscapes Dataset for Semantic Urban Scene Understanding, April 2016b. arXiv:1604.01685 [cs].

Chris Cremer. Inference suboptimality in variational autoencoders. *arXiv preprint arXiv:1801.03558*, 2018.

Marco Cuturi. Sinkhorn distances: Lightspeed computation of optimal transport. *NeurIPS*, 26, 2013.

Steffen Czolbe, Kasra Arnavaz, Oswin Krause, and Aasa Feragen. Is segmentation uncertainty useful? In *Information Processing in Medical Imaging: 27th International Conference, IPMI 2021, Virtual Event, June 28–June 30, 2021, Proceedings* 27, pp. 715–726. Springer, 2021.

Lavsen Dahal, Aayush Kafle, and Bishesh Khanal. Uncertainty Estimation in Deep 2D Echocardiography Segmentation, May 2020. arXiv:2005.09349 [cs].

Erik Daxberger, Agustinus Kristiadi, Alexander Immer, Runa Eschenhagen, et al. Laplace redux – effortless bayesian deep learning. *arXiv preprint arXiv:2106.14806*, 2021.

Ivo Pascal de Jong, Andreea Ioana Sburlea, and Matias Valdenegro-Toro. How disentangled are your classification uncertainties? *arXiv preprint arXiv:2408.12175*, 2024.

Clément Dechesne, Pierre Lassalle, and Sébastien Lefèvre. Bayesian u-net: Estimating uncertainty in semantic segmentation of earth observation images. *Remote Sensing*, 13(19):3836, 2021.

A Dempster. Upper and lower probabilities induced by multivalued mapping, a. of mathematical statistics, ed. *AMS-38*, 10, 1967.

Stefan Depeweg, Jose-Miguel Hernandez-Lobato, Finale Doshi-Velez, and Steffen Udluft. Decomposition of uncertainty in bayesian deep learning for efficient and risk-sensitive learning. In *International conference on machine learning*, pp. 1184–1193. PMLR, 2018.

Armen Der Kiureghian and Ove Ditlevsen. Aleatory or epistemic? does it matter? *Structural safety*, 31(2): 105–112, 2009.

Terrance DeVries and Graham W Taylor. Leveraging uncertainty estimates for predicting segmentation quality. *arXiv preprint arXiv:1807.00502*, 2018.

Nameirakpam Dhanachandra, Khumanthem Manglem, and Yambem Jina Chanu. Image segmentation using k -means clustering algorithm and subtractive clustering algorithm. *Procedia Computer Science*, 54:764–771, 2015.

Zhipeng Ding, Xu Han, Peirong Liu, and Marc Niethammer. Local Temperature Scaling for Probability Calibration, July 2021. arXiv:2008.05105 [cs].

Alexey Dosovitskiy, Lucas Beyer, Alexander Kolesnikov, Dirk Weissenborn, Xiaohua Zhai, Thomas Unterthiner, Mostafa Dehghani, Matthias Minderer, Georg Heigold, Sylvain Gelly, et al. An image is worth 16x16 words: Transformers for image recognition at scale. *arXiv preprint arXiv:2010.11929*, 2020.

Zach Eaton-Rosen, Felix Bragman, Sotirios Bisdas, Sébastien Ourselin, and M Jorge Cardoso. Towards safe deep learning: accurately quantifying biomarker uncertainty in neural network predictions. In *MICCAI*, pp. 691–699. Springer, 2018.

Matthias Eisenmann, Annika Reinke, and Vivien Weru. Why is the winner the best? *ArXiv*, abs/2303.17719, 2023.

Michael Havbro Faber. On the treatment of uncertainties and probabilities in engineering decision analysis. 2005.

Mário Figueiredo. Adaptive sparseness using jeffreys prior. *NeurIPS*, 14, 2001.

Paul Fischer, K Thomas, and Christian F Baumgartner. Uncertainty estimation and propagation in accelerated mri reconstruction. In *UNSURE workshop, MICCAI*, pp. 84–94. Springer, 2023.

Loic Le Folgoc, Vasileios Baltatzis, Sujal Desai, Anand Devaraj, Sam Ellis, Octavio E Martinez Manzanera, Arjun Nair, Huaqi Qiu, Julia Schnabel, and Ben Glocker. Is mc dropout bayesian? *arXiv preprint arXiv:2110.04286*, 2021.

Mélanie Gaillotchet, Christian Desrosiers, and Hervé Lombaert. Active learning for medical image segmentation with stochastic batches. *Medical Image Analysis*, 90:102958, 2023.

Yarin Gal and Zoubin Ghahramani. Dropout as a bayesian approximation: Representing model uncertainty in deep learning. In *ICML*, pp. 1050–1059. PMLR, 2016.

Yarin Gal, Jiri Hron, and Alex Kendall. Concrete dropout. *NeurIPS*, 30, 2017a.

Yarin Gal, Riashat Islam, and Zoubin Ghahramani. Deep bayesian active learning with image data. In *International conference on machine learning*, pp. 1183–1192. PMLR, 2017b.

Marc Gantzenbein, Ertunc Erdil, and Ender Konukoglu. Revphise: A memory-efficient neural network for uncertainty quantification in medical image segmentation. In *UNSURE workshop, MICCAI*, pp. 13–22. Springer, 2020.

Zhitong Gao, Yucong Chen, Chuyu Zhang, and Xuming He. Modeling multimodal aleatoric uncertainty in segmentation with mixture of stochastic expert. *arXiv preprint arXiv:2212.07328*, 2022.

Carlos García Rodríguez, Jordi Vitrià, and Oscar Mora. Uncertainty-based human-in-the-loop deep learning for land cover segmentation. *Remote Sensing*, 12(22):3836, 2020.

Lizeth Gonzalez-Carabarin, Iris AM Huijben, Bastian Veeling, Alexandre Schmid, and Ruud JG van Sloun. Dynamic probabilistic pruning: A general framework for hardware-constrained pruning at different granularities. *IEEE Transactions on Neural Networks and Learning Systems*, 35(1):733–744, 2022.

Ian Goodfellow, Jean Pouget-Abadie, Mehdi Mirza, Bing Xu, David Warde-Farley, Sherjil Ozair, Aaron Courville, and Yoshua Bengio. Generative adversarial nets. *NeurIPS*, 27, 2014.

Marc Gorriz, Axel Carlier, Emmanuel Faure, and Xavier Giro-i Nieto. Cost-effective active learning for melanoma segmentation. *arXiv preprint arXiv:1711.09168*, 2017.

Karol Gregor, Ivo Danihelka, Alex Graves, Danilo Rezende, and Daan Wierstra. Draw: A recurrent neural network for image generation. In *ICML*, pp. 1462–1471. PMLR, 2015.

Arthur Gretton, Karsten M Borgwardt, Malte J Rasch, Bernhard Schölkopf, and Alexander Smola. A kernel two-sample test. *The Journal of Machine Learning Research*, 13(1):723–773, 2012.

Chuan Guo, Geoff Pleiss, Yu Sun, and Kilian Q Weinberger. On calibration of modern neural networks. In *ICML*, pp. 1321–1330. PMLR, 2017.

Evan Hann, Iulia A. Popescu, Qiang Zhang, Ricardo A. Gonzales, Ahmet Barutçu, Stefan Neubauer, Vanessa M. Ferreira, and Stefan K. Piechnik. Deep neural network ensemble for on-the-fly quality control-driven segmentation of cardiac MRI T1 mapping. *Medical Image Analysis*, 71:102029, July 2021. ISSN 13618415. doi: 10.1016/j.media.2021.102029.

SM Kamrul Hasan and Cristian A Linte. Calibration of cine mri segmentation probability for uncertainty estimation using a multi-task cross-task learning architecture. In *Medical Imaging 2022: Image-Guided Procedures, Robotic Interventions, and Modeling*, volume 12034, pp. 174–179. SPIE, 2022a.

SM Kamrul Hasan and Cristian A Linte. Joint segmentation and uncertainty estimation of ventricular structures from cardiac mri using a bayesian condenseunet. In *2022 44th Annual International Conference of the IEEE Engineering in Medicine & Biology Society (EMBC)*, pp. 5047–5050. IEEE, 2022b.

Leonard Hasenclever, Stefan Webb, Thibaut Lienart, Sebastian Vollmer, Balaji Lakshminarayanan, Charles Blundell, and Yee Whye Teh. Distributed bayesian learning with stochastic natural gradient expectation propagation and the posterior server. *The Journal of Machine Learning Research*, 18(1):3744–3780, 2017.

Xu Owen He. Mixture of a million experts. *arXiv preprint arXiv:2407.04153*, 2024.

Jon C Helton. Uncertainty and sensitivity analysis in the presence of stochastic and subjective uncertainty. *journal of statistical computation and simulation*, 57(1-4):3–76, 1997.

José Miguel Hernández-Lobato and Ryan Adams. Probabilistic backpropagation for scalable learning of bayesian neural networks. In *ICML*, pp. 1861–1869. PMLR, 2015.

Yuta Hiasa, Yoshito Otake, Masaki Takao, Takeshi Ogawa, Nobuhiko Sugano, and Yoshinobu Sato. Automated muscle segmentation from clinical ct using bayesian u-net for personalized musculoskeletal modeling. *IEEE transactions on medical imaging*, 39(4):1030–1040, 2019.

Irina Higgins, Loic Matthey, Arka Pal, Christopher P Burgess, Xavier Glorot, Matthew M Botvinick, Shakir Mohamed, and Alexander Lerchner. beta-vae: Learning basic visual concepts with a constrained variational framework. *ICLR (Poster)*, 3, 2017.

Jonathan Ho, Ajay Jain, and Pieter Abbeel. Denoising diffusion probabilistic models. *NeurIPS*, 33:6840–6851, 2020.

Katharina Hoebel, Ken Chang, Jay Patel, Praveer Singh, and Jayashree Kalpathy-Cramer. Give me (un)certainty – An exploration of parameters that affect segmentation uncertainty, November 2019. *arXiv:1911.06357 [cs, eess]*.

Katharina Hoebel, Vincent Andrearczyk, Andrew L. Beers, Jay B. Patel, Ken Chang, Adrien Depeursinge, Henning Mueller, and Jayashree Kalpathy-Cramer. An exploration of uncertainty information for segmentation quality assessment. In Bennett A. Landman and Ivana Išgum (eds.), *Medical Imaging 2020: Image Processing*, pp. 55, Houston, United States, March 2020. SPIE. ISBN 978-1-5106-3393-3 978-1-5106-3394-0. doi: 10.1117/12.2548722.

Katharina Hoebel, Christopher Bridge, Andreeanne Lemay, Ken Chang, Jay Patel, Bruce Rosen, and Jayashree Kalpathy-Cramer. Do i know this? segmentation uncertainty under domain shift. In *Medical Imaging 2022: Image Processing*, volume 12032, pp. 261–276. SPIE, 2022.

Christopher J Holder and Muhammad Shafique. Efficient uncertainty estimation in semantic segmentation via distillation. In *Proceedings of the IEEE/CVF International Conference on Computer Vision*, pp. 3087–3094, 2021.

Emiel Hoogeboom, Didrik Nielsen, Priyank Jaini, Patrick Forré, and Max Welling. Argmax flows and multinomial diffusion: Learning categorical distributions. *NeurIPS*, 34:12454–12465, 2021.

Neil Houlsby, Ferenc Huszár, Zoubin Ghahramani, and Máté Lengyel. Bayesian active learning for classification and preference learning. *arXiv preprint arXiv:1112.5745*, 2011.

Neil Houlsby, José Miguel Hernández-Lobato, and Zoubin Ghahramani. Cold-start active learning with robust ordinal matrix factorization. In *International conference on machine learning*, pp. 766–774. PMLR, 2014.

Andrew Howard, Mark Sandler, Grace Chu, Liang-Chieh Chen, Bo Chen, Mingxing Tan, Weijun Wang, Yukun Zhu, Ruoming Pang, Vijay Vasudevan, et al. Searching for mobilenetv3. In *IEEE/CVF ICCV*, pp. 1314–1324, 2019.

Qingqiao Hu, Hao Wang, Jing Luo, Yunhao Luo, Zhiheng Zhang, Jan S Kirschke, Benedikt Wiestler, Bjoern Menze, Jianguo Zhang, and Hongwei Bran Li. Inter-rater uncertainty quantification in medical image segmentation via rater-specific bayesian neural networks. *arXiv preprint arXiv:2306.16556*, 2023.

Shi Hu, Daniel Worrall, Stefan Knegt, Bas Veeling, Henkjan Huisman, and Max Welling. Supervised Uncertainty Quantification for Segmentation with Multiple Annotations, May 2022. *arXiv:1907.01949 [cs, stat]*.

Gao Huang, Yixuan Li, Geoff Pleiss, Zhuang Liu, John E Hopcroft, and Kilian Q Weinberger. Snapshot ensembles: Train 1, get m for free. *arXiv preprint arXiv:1704.00109*, 2017.

Po-Yu Huang, Wan-Ting Hsu, Chun-Yueh Chiu, Ting-Fan Wu, and Min Sun. Efficient uncertainty estimation for semantic segmentation in videos. In *ECCV*, pp. 520–535, 2018.

Iris AM Huijben, Wouter Kool, Max B Paulus, and Ruud JG Van Sloun. A review of the gumbel-max trick and its extensions for discrete stochasticity in machine learning. *IEEE Trans. Pattern Anal. Mach. Intell.*, 45(2):1353–1371, 2022.

Eyke Hüllermeier and Willem Waegeman. Aleatoric and epistemic uncertainty in machine learning: An introduction to concepts and methods. *Machine Learning*, 110:457–506, 2021.

Fabian Isensee, Paul F. Jaeger, Simon A. A. Kohl, Jens Petersen, and Klaus Maier-Hein. nnu-net: a self-configuring method for deep learning-based biomedical image segmentation. *Nature Methods*, 18:203 – 211, 2020.

Fabian Isensee, Tassilo Wald, Constantin Ulrich, Michael Baumgartner, Saikat Roy, Klaus Maier-Hein, and Paul F Jaeger. nnu-net revisited: A call for rigorous validation in 3d medical image segmentation. *arXiv preprint arXiv:2404.09556*, 2024.

Phillip Isola, Jun-Yan Zhu, Tinghui Zhou, and Alexei A Efros. Image-to-image translation with conditional adversarial networks. In *IEEE/CVF CVPR*, pp. 1125–1134, 2017.

Sora Iwamoto, Bisser Raytchev, Toru Tamaki, and Kazufumi Kaneda. Improving the reliability of semantic segmentation of medical images by uncertainty modeling with bayesian deep networks and curriculum learning. In *UNSURE workshop, MICCAI*, pp. 34–43. Springer, 2021.

Robert A Jacobs, Michael I Jordan, Steven J Nowlan, and Geoffrey E Hinton. Adaptive mixtures of local experts. *Neural computation*, 3(1):79–87, 1991.

Eric Jang, Shixiang Gu, and Ben Poole. Categorical reparameterization with gumbel-softmax. *arXiv preprint arXiv:1611.01144*, 2016.

Martin Holm Jensen, Dan Richter Jørgensen, Raluca Jalaboi, Mads Eiler Hansen, and Martin Aastrup Olsen. Improving Uncertainty Estimation in Convolutional Neural Networks Using Inter-rater Agreement. In Dinggang Shen, Tianming Liu, Terry M. Peters, Lawrence H. Staib, Caroline Essert, Sean Zhou, Pew-Thian Yap, and Ali Khan (eds.), *MICCAI*, volume 11767, pp. 540–548. Springer International Publishing, Cham, 2019. ISBN 978-3-030-32250-2 978-3-030-32251-9. doi: 10.1007/978-3-030-32251-9_59. Series Title: Lecture Notes in Computer Science.

Wei Ji, Shuang Yu, Junde Wu, Kai Ma, Cheng Bian, Qi Bi, Jingjing Li, Hanruo Liu, Li Cheng, and Yefeng Zheng. Learning Calibrated Medical Image Segmentation via Multi-rater Agreement Modeling. In *2021 IEEE/CVF Conference on Computer Vision and Pattern Recognition (CVPR)*, pp. 12336–12346, Nashville, TN, USA, June 2021. IEEE. ISBN 978-1-66544-509-2. doi: 10.1109/CVPR46437.2021.01216.

Alain Jungo and Mauricio Reyes. Assessing reliability and challenges of uncertainty estimations for medical image segmentation. In *MICCAI*, pp. 48–56. Springer, 2019.

Alain Jungo, Richard McKinley, Raphael Meier, Urspeter Knecht, Luis Vera, Julián Pérez-Beteta, David Molina-García, Víctor M Pérez-García, Roland Wiest, and Mauricio Reyes. Towards uncertainty-assisted brain tumor segmentation and survival prediction. In *BrainLes workshop, MICCAI*, pp. 474–485. Springer, 2018a.

Alain Jungo, Raphael Meier, Ekin Ermis, Evelyn Herrmann, and Mauricio Reyes. Uncertainty-driven sanity check: application to postoperative brain tumor cavity segmentation. *arXiv preprint arXiv:1806.03106*, 2018b.

Alain Jungo, Fabian Balsiger, and Mauricio Reyes. Analyzing the quality and challenges of uncertainty estimations for brain tumor segmentation. *Frontiers in neuroscience*, 14:501743, 2020.

Ata Kaban. On bayesian classification with laplace priors. *Pattern Recognition Letters*, 28(10):1271–1282, 2007.

Kim-Celine Kahl, Carsten T Lüth, Maximilian Zenk, Klaus Maier-Hein, and Paul F Jaeger. Values: A framework for systematic validation of uncertainty estimation in semantic segmentation. *arXiv preprint arXiv:2401.08501*, 2024.

Konstantinos Kamnitsas, Wenjia Bai, Enzo Ferrante, Steven McDonagh, Matthew Sinclair, Nick Pawlowski, Martin Rajchl, Matthew Lee, Bernhard Kainz, Daniel Rueckert, et al. Ensembles of multiple models and architectures for robust brain tumour segmentation. In *BrainLes workshop, MICCAI*, pp. 450–462. Springer, 2018.

Michael Kampffmeyer, Arnt-Borre Salberg, and Robert Jenssen. Semantic segmentation of small objects and modeling of uncertainty in urban remote sensing images using deep convolutional neural networks. In *IEEE/CVF CVPR*, pp. 1–9, 2016.

Tejaswi Kasarla, Gattigorla Nagendar, Guruprasad M Hegde, Vineeth Balasubramanian, and CV Jawahar. Region-based active learning for efficient labeling in semantic segmentation. In *2019 IEEE winter conference on applications of computer vision (WACV)*, pp. 1109–1117. IEEE, 2019.

Michael Kass, Andrew P. Witkin, and Demetri Terzopoulos. Snakes: Active contour models. *IJCV*, 1: 321–331, 2004.

Elias Kassapis, Georgi Dikov, Deepak K. Gupta, and Cedric Nugteren. Calibrated Adversarial Refinement for Stochastic Semantic Segmentation, August 2021. *arXiv:2006.13144 [cs]*.

Alex Kendall and Yarin Gal. What uncertainties do we need in bayesian deep learning for computer vision? In *NeurIPS*, 2017.

Alex Kendall, Vijay Badrinarayanan, and Roberto Cipolla. Bayesian SegNet: Model Uncertainty in Deep Convolutional Encoder-Decoder Architectures for Scene Understanding, October 2016. *arXiv:1511.02680 [cs]*.

Nadieh Khalili, Joey Spronck, Francesco Ciompi, Jeroen van der Laak, and Geert Litjens. Uncertainty-guided annotation enhances segmentation with the human-in-the-loop. *arXiv preprint arXiv:2404.07208*, 2024.

Kwanyoung Kim, Dongwon Park, Kwang In Kim, and Se Young Chun. Task-aware variational adversarial active learning. In *Proceedings of the IEEE/CVF conference on computer vision and pattern recognition*, pp. 8166–8175, 2021.

Diederik P Kingma and Max Welling. Auto-encoding variational bayes. *arXiv preprint arXiv:1312.6114*, 2013.

Durk P Kingma, Tim Salimans, and Max Welling. Variational dropout and the local reparameterization trick. *NeurIPS*, 28, 2015.

Durk P Kingma, Tim Salimans, Rafal Jozefowicz, Xi Chen, Ilya Sutskever, and Max Welling. Improved variational inference with inverse autoregressive flow. *NeurIPS*, 29, 2016.

Michael Kirchhof, Gjergji Kasneci, and Enkelejda Kasneci. Reexamining the aleatoric and epistemic uncertainty dichotomy. In *ICLR Blogposts 2025*, 2025. URL <https://iclr-blogposts.github.io/2025/blog/reexamining-the-aleatoric-and-epistemic-uncertainty-dichotomy/>. <https://iclr-blogposts.github.io/2025/blog/reexamining-the-aleatoric-and-epistemic-uncertainty-dichotomy/>.

Andreas Kirsch. (implicit) ensembles of ensembles: Epistemic uncertainty collapse in large models. *arXiv preprint arXiv:2409.02628*, 2024.

Andreas Kirsch, Joost Van Amersfoort, and Yarin Gal. Batchbald: Efficient and diverse batch acquisition for deep bayesian active learning. *Advances in neural information processing systems*, 32, 2019.

Alexej Klushyn, Nutan Chen, Richard Kurle, Botond Cseke, and Patrick van der Smagt. Learning hierarchical priors in vaes. *NeurIPS*, 32, 2019.

Simon A. A. Kohl, Bernardino Romera-Paredes, Klaus H. Maier-Hein, Danilo Jimenez Rezende, S. M. Ali Eslami, Pushmeet Kohli, Andrew Zisserman, and Olaf Ronneberger. A Hierarchical Probabilistic U-Net for Modeling Multi-Scale Ambiguities, May 2019a. arXiv:1905.13077 [cs].

Simon A. A. Kohl, Bernardino Romera-Paredes, Clemens Meyer, Jeffrey De Fauw, Joseph R. Ledsam, Klaus H. Maier-Hein, S. M. Ali Eslami, Danilo Jimenez Rezende, and Olaf Ronneberger. A Probabilistic U-Net for Segmentation of Ambiguous Images, January 2019b. arXiv:1806.05034 [cs, stat].

Anoop Korattikara Balan, Vivek Rathod, Kevin P Murphy, and Max Welling. Bayesian dark knowledge. *NeurIPS*, 28, 2015.

Alex Krizhevsky, Ilya Sutskever, and Geoffrey E Hinton. Imagenet classification with deep convolutional neural networks. *NeurIPS*, 25, 2012.

Yongchan Kwon, Joong-Ho Won, Beom Joon Kim, and Myunghee Cho Paik. Uncertainty quantification using bayesian neural networks in classification: Application to biomedical image segmentation. *Computational Statistics & Data Analysis*, 142:106816, 2020.

Tyler LaBonte, Carianne Martinez, and Scott A Roberts. We know where we don't know: 3d bayesian cnns for credible geometric uncertainty. *arXiv preprint arXiv:1910.10793*, 2019.

Balaji Lakshminarayanan. *Decision trees and forests: a probabilistic perspective*. PhD thesis, UCL (University College London), 2016.

Balaji Lakshminarayanan, Alexander Pritzel, and Charles Blundell. Simple and scalable predictive uncertainty estimation using deep ensembles. *NeurIPS*, 30, 2017.

Benjamin Lambert, Florence Forbes, Senan Doyle, Alan Tucholka, and Michel Dojat. Improving uncertainty-based out-of-distribution detection for medical image segmentation. *arXiv preprint arXiv:2211.05421*, 2022.

Pierre-Simon Laplace. *Mémoires de Mathématique et de Physique, Tome Sixième*. l'Académie Royale des Sciences, 1774.

Agostina Larrazabal, Cesar Martinez, Jose Dolz, and Enzo Ferrante. Maximum entropy on erroneous predictions (meep): Improving model calibration for medical image segmentation. *arXiv preprint arXiv:2112.12218*, 2021a.

Agostina J Larrazabal, César Martínez, Jose Dolz, and Enzo Ferrante. Orthogonal ensemble networks for biomedical image segmentation. In *International Conference on Medical Image Computing and Computer-Assisted Intervention*, pp. 594–603. Springer, 2021b.

Yann LeCun, Léon Bottou, Yoshua Bengio, and Patrick Haffner. Gradient-based learning applied to document recognition. *Proceedings of the IEEE*, 86(11):2278–2324, 1998.

Bo Li and Tommy Sonne Alstrøm. On uncertainty estimation in active learning for image segmentation. *arXiv preprint arXiv:2007.06364*, 2020.

Yan Li, Xiaoyi Chen, Li Quan, and Ni Zhang. Uncertainty-guided robust training for medical image segmentation. In *2021 IEEE 18th International Symposium on Biomedical Imaging (ISBI)*, pp. 1471–1475. IEEE, 2021.

Tsung-Yi Lin, Michael Maire, Serge J. Belongie, James Hays, Pietro Perona, Deva Ramanan, Piotr Dollár, and C. Lawrence Zitnick. Microsoft coco: Common objects in context. In *ECCV*, 2014.

Jasper Linmans, Jeroen van der Laak, and Geert Litjens. Efficient out-of-distribution detection in digital pathology using multi-head convolutional neural networks. In *MDL*, pp. 465–478, 2020.

Yaron Lipman, Ricky TQ Chen, Heli Ben-Hamu, Maximilian Nickel, and Matt Le. Flow matching for generative modeling. *arXiv preprint arXiv:2210.02747*, 2022.

Bingyuan Liu, Ismail Ben Ayed, Adrian Galdran, and Jose Dolz. The Devil is in the Margin: Margin-based Label Smoothing for Network Calibration, March 2022a. arXiv:2111.15430 [cs].

Jeremiah Liu, Zi Lin, Shreyas Padhy, Dustin Tran, Tania Bedrax Weiss, and Balaji Lakshminarayanan. Simple and principled uncertainty estimation with deterministic deep learning via distance awareness. *Advances in neural information processing systems*, 33:7498–7512, 2020.

Jie Liu, Pan Zhou, Zehao Xiao, Jiayi Shen, Wenzhe Yin, Jan-Jakob Sonke, and Efstratios Gavves. Probabilistic interactive 3d segmentation with hierarchical neural processes. *arXiv preprint arXiv:2505.01726*, 2025.

Xiaofeng Liu, Fangxu Xing, Thibault Marin, Georges El Fakhri, and Jonghye Woo. Variational Inference for Quantifying Inter-observer Variability in Segmentation of Anatomical Structures, January 2022b. arXiv:2201.07106 [cs].

Zhuang Liu, Hanzi Mao, Chao-Yuan Wu, Christoph Feichtenhofer, Trevor Darrell, and Saining Xie. A convnet for the 2020s. In *IEEE/CVF CVPR*, pp. 11976–11986, 2022c.

Xiaojiang Long, Wei Chen, Qiuli Wang, Xiaohong Zhang, Chen Liu, Yucong Li, and Jiuquan Zhang. A probabilistic model for segmentation of ambiguous 3d lung nodule. In *IEEE ICASSP*, pp. 1130–1134. IEEE, 2021a.

Xiaojiang Long, Wei Chen, Qiuli Wang, Xiaohong Zhang, Chen Liu, Yucong Li, and Jiuquan Zhang. A Probabilistic Model for Segmentation of Ambiguous 3D Lung Nodule. In *ICASSP 2021 - 2021 IEEE International Conference on Acoustics, Speech and Signal Processing (ICASSP)*, pp. 1130–1134, Toronto, ON, Canada, June 2021b. IEEE. ISBN 978-1-72817-605-5. doi: 10.1109/ICASSP39728.2021.9415006.

Christos Louizos and Max Welling. Structured and efficient variational deep learning with matrix gaussian posteriors. In *ICML*, pp. 1708–1716. PMLR, 2016.

Calvin Luo. Understanding diffusion models: A unified perspective. *arXiv preprint arXiv:2208.11970*, 2022.

Carsten Lüth, Till Bungert, Lukas Klein, and Paul Jaeger. Navigating the pitfalls of active learning evaluation: A systematic framework for meaningful performance assessment. *Advances in Neural Information Processing Systems*, 36:9789–9836, 2023.

Siteng Ma, Prateek Mathur, Zheng Ju, Aonghus Lawlor, and Ruihai Dong. Model-data-driven adversarial active learning for brain tumor segmentation. *Computers in Biology and Medicine*, 176:108585, 2024a.

Siteng Ma, Haochang Wu, Aonghus Lawlor, and Ruihai Dong. Breaking the barrier: Selective uncertainty-based active learning for medical image segmentation. *arXiv preprint arXiv:2401.16298*, 2024b.

David John Cameron Mackay. *Bayesian methods for adaptive models*. California Institute of Technology, 1992.

Chris J. Maddison, Andriy Mnih, and Yee Whye Teh. The concrete distribution: A continuous relaxation of discrete random variables. *arXiv preprint arXiv:1611.00712*, 2016.

Dwarikanath Mahapatra, Behzad Bozorgtabar, Jean-Philippe Thiran, and Mauricio Reyes. Efficient active learning for image classification and segmentation using a sample selection and conditional generative adversarial network. In *International Conference on Medical Image Computing and Computer-Assisted Intervention*, pp. 580–588. Springer, 2018.

James Martens and Roger Grosse. Optimizing neural networks with kronecker-factored approximate curvature. In *Proceedings of the 32nd International Conference on Machine Learning (ICML)*, 2015.

Brian McCrindle, Katherine Zukotynski, Thomas E Doyle, and Michael D Noseworthy. A radiology-focused review of predictive uncertainty for ai interpretability in computer-assisted segmentation. *Radiology: Artificial Intelligence*, 3(6):e210031, 2021.

Alireza Mehrtash, William M. Wells, Clare M. Tempany, Purang Abolmaesumi, and Tina Kapur. Confidence Calibration and Predictive Uncertainty Estimation for Deep Medical Image Segmentation. *IEEE Trans. Med. Imag.*, 39(12):3868–3878, December 2020. ISSN 0278-0062, 1558-254X. doi: 10.1109/TMI.2020.3006437.

Chenlin Meng, Robin Rombach, Ruiqi Gao, Diederik Kingma, Stefano Ermon, Jonathan Ho, and Tim Salimans. On distillation of guided diffusion models. In *Proceedings of the IEEE/CVF Conference on Computer Vision and Pattern Recognition*, pp. 14297–14306, 2023.

Shervin Minaee and Yao Wang. An admm approach to masked signal decomposition using subspace representation. *IEEE IEEE Trans. Image Process*, 28:3192–3204, 2017.

Shervin Minaee, Yuri Boykov, Fatih Murat Porikli, Antonio J. Plaza, Nasser Kehtarnavaz, and Demetri Terzopoulos. Image segmentation using deep learning: A survey. *IEEE Trans. Pattern Anal. Mach. Intell.*, 44:3523–3542, 2020.

Thomas P Minka. Bayesian model averaging is not model combination. *Available electronically at <http://www.stat.cmu.edu/minka/papers/bma.html>*, pp. 1–2, 2000.

Sudhanshu Mittal, Maxim Tatarchenko, Özgün Çiçek, and Thomas Brox. Parting with illusions about deep active learning. *arXiv preprint arXiv:1912.05361*, 2019.

Aryan Mobiny, Pengyu Yuan, Supratik K Moulik, Naveen Garg, Carol C Wu, and Hien Van Nguyen. Dropconnect is effective in modeling uncertainty of bayesian deep networks. *Scientific reports*, 11(1):5458, 2021.

Miguel Monteiro, Loic Le Folgoc, Daniel Coelho de Castro, Nick Pawlowski, Bernardo Marques, Konstantinos Kamnitsas, Mark van der Wilk, and Ben Glocker. Stochastic Segmentation Networks: Modelling Spatially Correlated Aleatoric Uncertainty. In *NeurIPS*, volume 33, pp. 12756–12767. Curran Associates, Inc., 2020.

D Morrison, A Milan, and E Antonakos. Uncertainty-aware instance segmentation using dropout sampling. In *Proceedings of the Robotic Vision Probabilistic Object Detection Challenge (CVPR 2019 Workshop), Long Beach, CA, USA*, pp. 16–20, 2019.

Luca Mossina, Joseba Dalmau, and Léo Andéol. Conformal semantic image segmentation: Post-hoc quantification of predictive uncertainty. In *Proceedings of the IEEE/CVF Conference on Computer Vision and Pattern Recognition*, pp. 3574–3584, 2024.

Bálint Mucsányi, Michael Kirchhof, and Seong Joon Oh. Benchmarking uncertainty disentanglement: Specialized uncertainties for specialized tasks. *Advances in neural information processing systems*, 37:50972–51038, 2024.

Jishnu Mukhoti and Yarin Gal. Evaluating bayesian deep learning methods for semantic segmentation. *arXiv preprint arXiv:1811.12709*, 2018.

Jishnu Mukhoti, Viveka Kulharia, Amartya Sanyal, Stuart Golodetz, Philip Torr, and Puneet Dokania. Calibrating deep neural networks using focal loss. *NeurIPS*, 33:15288–15299, 2020.

Jishnu Mukhoti, Andreas Kirsch, Joost van Amersfoort, Philip HS Torr, and Yarin Gal. Deep deterministic uncertainty: A new simple baseline. In *IEEE/CVF CVPR*, pp. 24384–24394, 2023.

Prateek Munjal, Nasir Hayat, Munawar Hayat, Jamshid Sourati, and Shadab Khan. Towards robust and reproducible active learning using neural networks. In *Proceedings of the IEEE/CVF Conference on Computer Vision and Pattern Recognition*, pp. 223–232, 2022.

Tanya Nair, Doina Precup, Douglas L Arnold, and Tal Arbel. Exploring uncertainty measures in deep networks for multiple sclerosis lesion detection and segmentation. *Medical image analysis*, 59:101557, 2020.

Laurent Najman and Michel Schmitt. Watershed of a continuous function. *Signal Process.*, 38:99–112, 1994.

Vishwesh Nath, Dong Yang, Bennett A Landman, Daguang Xu, and Holger R Roth. Diminishing uncertainty within the training pool: Active learning for medical image segmentation. *IEEE Transactions on Medical Imaging*, 40(10):2534–2547, 2020.

Vishwesh Nath, Dong Yang, Holger R Roth, and Daguang Xu. Warm start active learning with proxy labels and selection via semi-supervised fine-tuning. In *International conference on medical image computing and computer-assisted intervention*, pp. 297–308. Springer, 2022.

Radford M Neal. *Bayesian learning for neural networks*, volume 118. Springer Science & Business Media, 2012.

Lukas Neumann, Andrew Zisserman, and Andrea Vedaldi. Relaxed softmax: Efficient confidence auto-calibration for safe pedestrian detection. 2018.

Matthew Ng, Fumin Guo, Labonny Biswas, Steffen E Petersen, Stefan K Piechnik, Stefan Neubauer, and Graham Wright. Estimating uncertainty in neural networks for cardiac mri segmentation: A benchmark study. *IEEE Trans. Biomed. Eng*, 2022.

Alexander Quinn Nichol and Prafulla Dhariwal. Improved denoising diffusion probabilistic models. In *ICML*, pp. 8162–8171. PMLR, 2021.

Richard Nock and Frank Nielsen. Statistical region merging. *IEEE Trans. Pattern Anal. Mach. Intell.*, 26: 1452–1458, 2004.

Hyeonwoo Noh, Seunghoon Hong, and Bohyung Han. Learning deconvolution network for semantic segmentation. *IEEE ICCV*, pp. 1520–1528, 2015.

Ian Osband. Risk versus uncertainty in deep learning: Bayes, bootstrap and the dangers of dropout. In *NeurIPS workshop on bayesian deep learning*, volume 192. MIT Press, 2016.

Nobuyuki Otsu. A threshold selection method from gray level histograms. *IEEE Transactions on Systems, Man, and Cybernetics*, 9:62–66, 1979.

Firat Ozdemir, Zixuan Peng, Philipp Fuernstahl, Christine Tanner, and Orcun Goksel. Active learning for segmentation based on bayesian sample queries. *Knowledge-Based Systems*, 214:106531, 2021.

Onur Ozdemir, Benjamin Woodward, and Andrew A Berlin. Propagating uncertainty in multi-stage bayesian convolutional neural networks with application to pulmonary nodule detection. *arXiv preprint arXiv:1712.00497*, 2017.

Theodore Papamarkou, Maria Skouliaridou, Konstantina Palla, Laurence Aitchison, Julyan Arbel, David Dunson, Maurizio Filippone, Vincent Fortuin, Philipp Hennig, José Miguel Hernández-Lobato, et al. Position: Bayesian deep learning is needed in the age of large-scale ai. *arXiv preprint arXiv:2402.00809*, 2024.

Svetlana Pavlitskaya, Christian Hubschneider, Michael Weber, Ruby Moritz, Fabian Huger, Peter Schlicht, and J. Marius Zollner. Using Mixture of Expert Models to Gain Insights into Semantic Segmentation. In *2020 IEEE/CVF Conference on Computer Vision and Pattern Recognition Workshops (CVPRW)*, pp. 1399–1406, Seattle, WA, USA, June 2020. IEEE. ISBN 978-1-72819-360-1. doi: 10.1109/CVPRW50498.2020.00179.

Gabriel Pereyra, George Tucker, Jan Chorowski, Łukasz Kaiser, and Geoffrey Hinton. Regularizing neural networks by penalizing confident output distributions. *arXiv preprint arXiv:1701.06548*, 2017.

Ben Philps, Maria del C. Valdes Hernandez, Susana Munoz Maniega, Mark E Bastin, Eleni Sakka, Una Clancy, Joanna M Wardlaw, and Miguel O Bernabeu. Stochastic uncertainty quantification techniques fail to account for inter-analyst variability in white matter hyperintensity segmentation. In *Annual Conference on Medical Image Understanding and Analysis*, pp. 34–53. Springer, 2024.

Nils Plath, Marc Toussaint, and Shinichi Nakajima. Multi-class image segmentation using conditional random fields and global classification. In *ICML*, 2009.

Janis Postels, Francesco Ferroni, Huseyin Coskun, Nassir Navab, and Federico Tombari. Sampling-free epistemic uncertainty estimation using approximated variance propagation. In *Proceedings of the IEEE/CVF international conference on computer vision*, pp. 2931–2940, 2019.

Chao Qi, Jianqin Yin, Yingchun Niu, and Jinghang Xu. Neighborhood spatial aggregation mc dropout for efficient uncertainty-aware semantic segmentation in point clouds. *IEEE Transactions on Geoscience and Remote Sensing*, 2023.

Di Qiu and Lok Ming Lui. Modal uncertainty estimation via discrete latent representation. *arXiv preprint arXiv:2007.12858*, 2020.

Xavier Rafael-Palou, Anton Aubanell, Mario Ceresa, Vicent Ribas, Gemma Piella, and Miguel A. González Ballester. An Uncertainty-aware Hierarchical Probabilistic Network for Early Prediction, Quantification and Segmentation of Pulmonary Tumour Growth, April 2021. arXiv:2104.08789 [cs].

Aimon Rahman, Jeya Maria Jose Valanarasu, Ilker Hacihaliloglu, and Vishal M. Patel. Ambiguous Medical Image Segmentation using Diffusion Models, April 2023. arXiv:2304.04745 [cs].

Marianne Rakic, Hallee E Wong, Jose Javier Gonzalez Ortiz, Beth A Cimini, John V Guttag, and Adrian V Dalca. Tyche: Stochastic in-context learning for medical image segmentation. In *IEEE/CVF CVPR*, pp. 11159–11173, 2024.

Rajesh Ranganath, Dustin Tran, and David Blei. Hierarchical variational models. In *ICML*, pp. 324–333. PMLR, 2016.

Pengzhen Ren, Yun Xiao, Xiaojun Chang, Po-Yao Huang, Zhihui Li, Brij B Gupta, Xiaojiang Chen, and Xin Wang. A survey of deep active learning. *ACM computing surveys (CSUR)*, 54(9):1–40, 2021.

Danilo Jimenez Rezende and Shakir Mohamed. Variational inference with normalizing flows. *arXiv preprint arXiv:1505.05770*, 2015.

Stephan R. Richter, Vibhav Vineet, Stefan Roth, and Vladlen Koltun. Playing for data: Ground truth from computer games. *ArXiv*, abs/1608.02192, 2016.

O. Ronneberger, P. Fischer, and T. Brox. U-net: Convolutional networks for biomedical image segmentation. In *MICCAI*, volume 9351 of *LNCS*, pp. 234–241. Springer, 2015.

Parinaz Roshanzamir, Hassan Rivaz, Joshua Ahn, Hamza Mirza, Neda Naghdi, Meagan Anstruther, Michele C Battié, Maryse Fortin, and Yiming Xiao. How inter-rater variability relates to aleatoric and epistemic uncertainty: a case study with deep learning-based paraspinal muscle segmentation. In *UNSURE workshop, MICCAI*, pp. 74–83. Springer, 2023.

Abhijit Guha Roy, Sailesh Conjeti, Nassir Navab, and Christian Wachinger. Bayesian quicknat: Model uncertainty in deep whole-brain segmentation for structure-wise quality control. *NeuroImage*, 195:11–22, 2018a.

Abhijit Guha Roy, Sailesh Conjeti, Nassir Navab, and Christian Wachinger. Inherent brain segmentation quality control from fully convnet monte carlo sampling. In *MICCAI*, pp. 664–672. Springer, 2018b.

Josef Lorenz Rumberger, Lisa Mais, and Dagmar Kainmueller. Probabilistic Deep Learning for Instance Segmentation. In Adrien Bartoli and Andrea Fusiello (eds.), *Computer Vision – ECCV 2020 Workshops*, volume 12535, pp. 445–457. Springer International Publishing, Cham, 2020a. ISBN 978-3-030-66414-5 978-3-030-66415-2. doi: 10.1007/978-3-030-66415-2_29. Series Title: Lecture Notes in Computer Science.

Josef Lorenz Rumberger, Lisa Mais, and Dagmar Kainmueller. Probabilistic deep learning for instance segmentation. In *ECCV*, pp. 445–457. Springer, 2020b.

Ario Sadafi, Niklas Koehler, Asya Makhro, Anna Bogdanova, Nassir Navab, Carsten Marr, and Tingying Peng. Multiclass deep active learning for detecting red blood cell subtypes in brightfield microscopy. In *Medical Image Computing and Computer Assisted Intervention–MICCAI 2019: 22nd International Conference, Shenzhen, China, October 13–17, 2019, Proceedings, Part I* 22, pp. 685–693. Springer, 2019.

Anindo Saha, Matin Hosseinzadeh, and Henkjan Huisman. Encoding clinical priori in 3d convolutional neural networks for prostate cancer detection in bpmri. *arXiv preprint arXiv:2011.00263*, 2020.

Anindo Saha, Joeran Bosma, Jasper Linmans, Matin Hosseinzadeh, and Henkjan Huisman. Anatomical and Diagnostic Bayesian Segmentation in Prostate MRI – Should Different Clinical Objectives Mandate Different Loss Functions?, October 2021a. arXiv:2110.12889 [cs, eess].

Anindo Saha, Matin Hosseinzadeh, and Henkjan Huisman. End-to-end prostate cancer detection in bpMRI via 3D CNNs: Effects of attention mechanisms, clinical priori and decoupled false positive reduction. *Medical Image Analysis*, 73:102155, October 2021b. ISSN 13618415.

Jörg Sander, Bob D de Vos, Jelmer M Wolterink, and Ivana Išgum. Towards increased trustworthiness of deep learning segmentation methods on cardiac mri. In *Medical imaging 2019: image Processing*, volume 10949, pp. 324–330. SPIE, 2019.

Chinmay Savadikar, Rahul Kulhalli, and Bhushan Garware. Brain tumour segmentation using probabilistic u-net. In *BrainLes workshop, MICCAI*, pp. 255–264. Springer, 2021.

Arne Schmidt, Pablo Morales-Álvarez, and Rafael Molina. Probabilistic modeling of inter-and intra-observer variability in medical image segmentation. In *IEEE/CVF ICCV*, pp. 21097–21106, 2023.

Suman Sedai, Bhavna Josephine Antony, Dwarikanath Mahapatra, and Rahil Garnavi. Joint segmentation and uncertainty visualization of retinal layers in optical coherence tomography images using bayesian deep learning. *ArXiv*, abs/1809.04282, 2018.

Philipp Seeböck, José Ignacio Orlando, Thomas Schlegl, Sebastian M. Waldstein, Hrvoje Bogunović, Sophie Klimscha, Georg Langs, and Ursula Margarethe Schmidt-Erfurth. Exploiting epistemic uncertainty of anatomy segmentation for anomaly detection in retinal oct. *IEEE Trans. Med. Imag.*, 39:87–98, 2019.

Raghavendra Selvan, Frederik Faye, Jon Middleton, and Akshay Pai. Uncertainty quantification in medical image segmentation with normalizing flows, August 2020. arXiv:2006.02683 [cs, stat].

Murat Sensoy, Lance Kaplan, and Melih Kandemir. Evidential deep learning to quantify classification uncertainty. *NeurIPS*, 31, 2018.

Burr Settles. Active learning literature survey, 2009.

J Shawe-Taylor. Kernel methods for pattern analysis. *Cambridge University Press google schola*, 2:181–201, 2004.

Evan Shelhamer, Jonathan Long, and Trevor Darrell. Fully convolutional networks for semantic segmentation. *IEEE/CVF CVPR*, pp. 3431–3440, 2014.

Maohao Shen, Jacky Y Zhang, Leihao Chen, Weiman Yan, Neel Jani, Brad Sutton, and Oluwasanmi Koyejo. Labeling cost sensitive batch active learning for brain tumor segmentation. In *2021 IEEE 18th International Symposium on Biomedical Imaging (ISBI)*, pp. 1269–1273. IEEE, 2021.

Yawar Siddiqui, Julien Valentin, and Matthias Nießner. Viewal: Active learning with viewpoint entropy for semantic segmentation. In *IEEE/CVF CVPR*, pp. 9433–9443, 2020.

João Lourenço Silva and Arlindo L. Oliveira. Using Soft Labels to Model Uncertainty in Medical Image Segmentation, September 2021. arXiv:2109.12622 [cs].

Karen Simonyan and Andrew Zisserman. Very deep convolutional networks for large-scale image recognition. *arXiv preprint arXiv:1409.1556*, 2014.

Samarth Sinha, Sayna Ebrahimi, and Trevor Darrell. Variational adversarial active learning. In *Proceedings of the IEEE/CVF international conference on computer vision*, 2019.

Casper Kaae Sønderby, Tapani Raiko, Lars Maaløe, Søren Kaae Sønderby, and Ole Winther. Ladder variational autoencoders. *NeurIPS*, 29, 2016.

Hwanjun Song, Minseok Kim, Dongmin Park, Yooju Shin, and Jae-Gil Lee. Learning From Noisy Labels With Deep Neural Networks: A Survey. *IEEE Trans. Neural Netw. Learn. Syst.*, pp. 1–19, 2022. ISSN 2162-237X, 2162-2388. doi: 10.1109/TNNLS.2022.3152527.

Jiaming Song, Chenlin Meng, and Stefano Ermon. Denoising diffusion implicit models. *arXiv preprint arXiv:2010.02502*, 2020.

Jamshid Sourati, Ali Gholipour, Jennifer G Dy, Sila Kurugol, and Simon K Warfield. Active deep learning with fisher information for patch-wise semantic segmentation. In *International Workshop on Deep Learning in Medical Image Analysis*, pp. 83–91. Springer, 2018.

Jost Tobias Springenberg, Aaron Klein, Stefan Falkner, and Frank Hutter. Bayesian optimization with robust bayesian neural networks. *NeurIPS*, 29, 2016.

Jean-Luc Starck, Michael Elad, and David L. Donoho. Image decomposition via the combination of sparse representations and a variational approach. *IEEE Trans. Image Process*, 14:1570–1582, 2005.

Christian Szegedy, Wei Liu, Yangqing Jia, Pierre Sermanet, Scott Reed, Dragomir Anguelov, Dumitru Erhan, Vincent Vanhoucke, and Andrew Rabinovich. Going deeper with convolutions (2014). *arXiv preprint arXiv:1409.4842*, 10, 2014.

Christian Szegedy, Vincent Vanhoucke, Sergey Ioffe, Jon Shlens, and Zbigniew Wojna. Rethinking the inception architecture for computer vision. In *IEEE/CVF CVPR*, pp. 2818–2826, 2016.

Richard Szeliski. Computer vision - algorithms and applications. In *Texts in Computer Science*, 2010.

Abhinav Valada, Johan Vertens, Ankit Dhall, and Wolfram Burgard. Adapnet: Adaptive semantic segmentation in adverse environmental conditions. In *2017 IEEE International Conference on Robotics and Automation (ICRA)*, pp. 4644–4651. IEEE, 2017.

Matias Valdenegro-Toro and Daniel Saromo Mori. A deeper look into aleatoric and epistemic uncertainty disentanglement. In *2022 IEEE/CVF Conference on Computer Vision and Pattern Recognition Workshops (CVPRW)*, pp. 1508–1516. IEEE, 2022.

Amaan Valiuddin, Christiaan Viviers, Ruud van Sloun, Peter de With, and Fons van der Sommen. Retaining informative latent variables in probabilistic segmentation. In *IEEE ICASSP*, pp. 5635–5639. IEEE, 2024a.

M. M. A. Valiuddin, Christiaan G. A. Viviers, Ruud J. G. Van Sloun, Peter H. N. De With, and Fons van der Sommen. Investigating and improving latent density segmentation models for aleatoric uncertainty quantification in medical imaging. *IEEE Trans. Med. Imag.*, pp. 1–1, 2024b. doi: 10.1109/TMI.2024.3445999.

MM Amaan Valiuddin, Christiaan GA Viviers, Ruud JG van Sloun, Peter HN de With, and Fons van der Sommen. Improving aleatoric uncertainty quantification in multi-annotated medical image segmentation with normalizing flows. In *UNSURE workshop, MICCAI*, pp. 75–88. Springer, 2021.

Joost Van Amersfoort, Lewis Smith, Yee Whye Teh, and Yarin Gal. Uncertainty estimation using a single deep deterministic neural network. In *International conference on machine learning*, pp. 9690–9700. PMLR, 2020.

Aäron Van Den Oord, Nal Kalchbrenner, and Koray Kavukcuoglu. Pixel recurrent neural networks. In *ICML*, pp. 1747–1756. PMLR, 2016.

Aaron Van Den Oord, Oriol Vinyals, et al. Neural discrete representation learning. *NeurIPS*, 30, 2017.

Christiaan Viviers, Mark Ramaekers, Amaan Valiuddin, Terese Hellström, Nick Tasios, John van der Ven, Igor Jacobs, Lotte Ewals, Joost Nederend, Misha Luyer, et al. Segmentation-based assessment of tumor-vessel involvement for surgical resectability prediction of pancreatic ductal adenocarcinoma. In *IEEE/CVF ICCV*, pp. 2421–2431, 2023a.

Christiaan Viviers, Amaan Valiuddin, Peter H. N. De With, and Fons Van Der Sommen. Probabilistic 3D segmentation for aleatoric uncertainty quantification in full 3D medical data. In Khan M. Iftekharuddin and Weijie Chen (eds.), *Medical Imaging 2023: Computer-Aided Diagnosis*, pp. 31, San Diego, United States, April 2023b. SPIE. ISBN 978-1-5106-6035-9 978-1-5106-6036-6. doi: 10.1117/12.2654255.

Christiaan GA Viviers, MM Amaan Valiuddin, Fons van der Sommen, et al. Probabilistic 3d segmentation for aleatoric uncertainty quantification in full 3d medical data. In *Medical Imaging 2023: Computer-Aided Diagnosis*, volume 12465, pp. 341–351. SPIE, 2023c.

Stefan Wager, Sida Wang, and Percy S Liang. Dropout training as adaptive regularization. *NeurIPS*, 26, 2013.

Guotai Wang, Wenqi Li, Michael Aertsen, Jan Deprest, Sébastien Ourselin, and Tom Vercauteren. Aleatoric uncertainty estimation with test-time augmentation for medical image segmentation with convolutional neural networks. *Neurocomputing*, 338:34–45, 2019a.

Guotai Wang, Wenqi Li, Sébastien Ourselin, and Tom Vercauteren. Automatic brain tumor segmentation using convolutional neural networks with test-time augmentation. In *BrainLes workshop, MICCAI*, pp. 61–72. Springer, 2019b.

Max Welling and Yee W Teh. Bayesian learning via stochastic gradient langevin dynamics. In *ICML*, pp. 681–688, 2011.

Luke Whitbread and Mark Jenkinson. Uncertainty categories in medical image segmentation: A study of source-related diversity. In *International Workshop on Uncertainty for Safe Utilization of Machine Learning in Medical Imaging*, pp. 26–35. Springer, 2022.

Kristoffer Wickstrøm, Michael Kampffmeyer, and Robert Jenssen. Uncertainty and interpretability in convolutional neural networks for semantic segmentation of colorectal polyps. *Medical image analysis*, 60: 101619, 2020.

Håkan Wieslander, Philip J Harrison, Gabriel Skogberg, Sonya Jackson, Markus Fridén, Johan Karlsson, Ola Spjuth, and Carolina Wählby. Deep learning with conformal prediction for hierarchical analysis of large-scale whole-slide tissue images. *IEEE journal of biomedical and health informatics*, 25(2):371–380, 2020.

Lisa Wimmer, Yusuf Sale, Paul Hofman, Bernd Bischl, and Eyke Hüllermeier. Quantifying aleatoric and epistemic uncertainty in machine learning: Are conditional entropy and mutual information appropriate measures? In *Uncertainty in artificial intelligence*, pp. 2282–2292. PMLR, 2023.

Julia Wolleb, Robin Sandkühler, Florentin Bieder, Philippe Valmaggia, and Philippe C. Cattin. Diffusion Models for Implicit Image Segmentation Ensembles, December 2021. arXiv:2112.03145 [cs].

Junde Wu, Huihui Fang, Fangxin Shang, Zhaowei Wang, Dalu Yang, Wenshuo Zhou, Yehui Yang, and Yanwu Xu. Learning self-calibrated optic disc and cup segmentation from multi-rater annotations, June 2022. arXiv:2206.05092 [cs, eess].

Junde Wu, Rao Fu, Huihui Fang, Yu Zhang, and Yanwu Xu. MedSegDiff-V2: Diffusion based Medical Image Segmentation with Transformer, January 2023a. arXiv:2301.11798 [cs, eess].

Junde Wu, Rao Fu, Huihui Fang, Yu Zhang, Yehui Yang, Haoyi Xiong, Huiying Liu, and Yanwu Xu. MedSegDiff: Medical Image Segmentation with Diffusion Probabilistic Model, January 2023b. arXiv:2211.00611 [cs].

Tsung-Han Wu, Yueh-Cheng Liu, Yu-Kai Huang, Hsin-Ying Lee, Hung-Ting Su, Ping-Chia Huang, and Winston H Hsu. Redal: Region-based and diversity-aware active learning for point cloud semantic segmentation. In *IEEE/CVF ICCV*, pp. 15510–15519, 2021.

Anna M Wundram, Paul Fischer, Michael Mühlbach, Lisa M Koch, and Christian F Baumgartner. Conformal performance range prediction for segmentation output quality control. In *International Workshop on Uncertainty for Safe Utilization of Machine Learning in Medical Imaging*, pp. 81–91. Springer, 2024a.

Anna M Wundram, Paul Fischer, Stephan Wunderlich, Hanna Faber, Lisa M Koch, Philipp Berens, and Christian F Baumgartner. Leveraging probabilistic segmentation models for improved glaucoma diagnosis: A clinical pipeline approach. In *Medical Imaging with Deep Learning*, 2024b.

Binhui Xie, Longhui Yuan, Shuang Li, Chi Harold Liu, and Xijing Cheng. Towards fewer annotations: Active learning via region impurity and prediction uncertainty for domain adaptive semantic segmentation. In *Proceedings of the IEEE/CVF conference on computer vision and pattern recognition*, pp. 8068–8078, 2022.

Enze Xie, Wenhui Wang, Zhiding Yu, Anima Anandkumar, Jose M Alvarez, and Ping Luo. Segformer: Simple and efficient design for semantic segmentation with transformers. *NeurIPS*, 34:12077–12090, 2021.

Jingjing Xie, Bing Xu, and Zhang Chuang. Horizontal and vertical ensemble with deep representation for classification. *arXiv preprint arXiv:1306.2759*, 2013.

Lin Yang, Yizhe Zhang, Jianxu Chen, Siyuan Zhang, and Danny Z Chen. Suggestive annotation: A deep active learning framework for biomedical image segmentation. In *Medical Image Computing and Computer Assisted Intervention- MICCAI 2017: 20th International Conference, Quebec City, QC, Canada, September 11-13, 2017, Proceedings, Part III* 20, pp. 399–407. Springer, 2017.

Michelle Yuan, Hsuan-Tien Lin, and Jordan Boyd-Graber. Cold-start active learning through self-supervised language modeling. *arXiv preprint arXiv:2010.09535*, 2020a.

Yuhui Yuan, Xilin Chen, and Jingdong Wang. Object-contextual representations for semantic segmentation. In *ECCV*, 2019.

Yuhui Yuan, Xilin Chen, and Jingdong Wang. Object-contextual representations for semantic segmentation. 2020b.

Lukas Zbinden, Lars Doorenbos, Theodoros Pissas, Adrian Thomas Huber, Raphael Sznitman, and Pablo Márquez-Neila. Stochastic Segmentation with Conditional Categorical Diffusion Models, April 2023.

Kilian Zepf, Eike Petersen, Jes Frellsen, and Aasa Feragen. That label's got style: Handling label style bias for uncertain image segmentation. *arXiv preprint arXiv:2303.15850*, 2023a.

Kilian Zepf, Selma Wanna, Marco Miani, Juston Moore, Jes Frellsen, Søren Hauberg, Frederik Warburg, and Aasa Feragen. Laplacian segmentation networks improve epistemic uncertainty quantification. *arXiv preprint arXiv:2303.13123*, 2023b.

Kilian Zepf, Jes Frellsen, and Aasa Feragen. Navigating uncertainty in medical image segmentation. In *2024 IEEE International Symposium on Biomedical Imaging (ISBI)*, pp. 1–5. IEEE, 2024.

Ge Zhang, Hao Dang, and Yulong Xu. Epistemic and aleatoric uncertainties reduction with rotation variation for medical image segmentation with convnets. *SN Applied Sciences*, 4(2):56, 2022a.

Qinglong Zhang and Yu-Bin Yang. Rest: An efficient transformer for visual recognition. *NeurIPS*, 34: 15475–15485, 2021.

Wei Zhang, Xiaohong Zhang, Sheng Huang, Yuting Lu, and Kun Wang. A probabilistic model for controlling diversity and accuracy of ambiguous medical image segmentation. In *Proceedings of the 30th ACM International Conference on Multimedia*, pp. 4751–4759, 2022b.

Wei Zhang, Xiaohong Zhang, Sheng Huang, Yuting Lu, and Kun Wang. PixelSeg: Pixel-by-Pixel Stochastic Semantic Segmentation for Ambiguous Medical Images. In *Proceedings of the 30th ACM International Conference on Multimedia*, pp. 4742–4750, Lisboa Portugal, October 2022c. ACM. ISBN 978-1-4503-9203-7. doi: 10.1145/3503161.3548060.

Wei Zhang, Xiaohong Zhang, Sheng Huang, Yuting Lu, and Kun Wang. A Probabilistic Model for Controlling Diversity and Accuracy of Ambiguous Medical Image Segmentation. In *Proceedings of the 30th ACM International Conference on Multimedia*, pp. 4751–4759, Lisboa Portugal, October 2022d. ACM. ISBN 978-1-4503-9203-7. doi: 10.1145/3503161.3548115.

Shengjia Zhao, Jiaming Song, and Stefano Ermon. Infovae: Information maximizing variational autoencoders. *arXiv preprint arXiv:1706.02262*, 2017.

Hongkai Zheng, Weili Nie, Arash Vahdat, Kamyar Azizzadenesheli, and Anima Anandkumar. Fast sampling of diffusion models via operator learning. In *International conference on machine learning*, pp. 42390–42402. PMLR, 2023.

Yijia Zheng, Tong He, Yixuan Qiu, and David P Wipf. Learning manifold dimensions with conditional variational autoencoders. *NeurIPS*, 35:34709–34721, 2022.